Negative coupling: the coincidence of premating isolating barriers can reduce reproductive isolation

Thomas G. Aubier[1,2*], Michael Kopp[3], Isaac J. Linn[2], Oscar Puebla[4,5], Marina Rafajlović [6,7], Maria R. Servedio[2]

* corresponding author

Affiliations:

1. Centre de Recherche sur la Biodiversité et l'Environnement (CRBE), Université de Toulouse, CNRS, IRD,Toulouse INP, Université Toulouse 3 – Paul Sabatier (UT3), Toulouse, France
2. Department of Biology, University of North Carolina at Chapel Hill, Chapel Hill, NC 27599, USA
3. Aix Marseille Université, CNRS, Centrale Marseille, I2M, UMR 7373, 3 Place Victor Hugo, 13331 Marseille Cedex 3, France
4. Leibniz Centre for Tropical Marine Research, 28359 Bremen, Germany
5. Institute for Chemistry and Biology of the Marine Environment (ICBM), 26111 Oldenburg, Germany
6. Department of Marine Sciences, University of Gothenburg, 405 30 Gothenburg, Sweden
7. Linnaeus Centre for Marine Evolutionary Biology, University of Gothenburg, 453 96 Strömstad, Sweden

Emails (respectively):

thomas.aubier@normalesup.org, michael.kopp@univ-amu.fr, ijlinn01@live.unc.edu, oscar.puebla@leibniz-zmt.de, marina.rafajlovic@marine.gu.se, servedio@email.unc.edu

Author contributions:

TGA and MRS coordinated and led the development of the model and the writing of this paper, with contributions from all authors. TGA performed all analyses.

Short title:

Negative coupling of reproductive barriers

Abstract:

Speciation can be mediated by a variety of reproductive barriers, and the interaction among different barriers has often been shown to enhance overall reproductive isolation, a process referred to as 'coupling'. Here, we analyze a population genetics model to study the establishment of linkage disequilibrium (LD) among loci involved in multiple premating barriers, an aspect that has received little theoretical attention to date. We consider a simple genetic framework underlying two distinct premating barriers, each encoded by a preference locus and its associated mating trait locus. We show that their interaction can lead to a decrease in overall reproductive isolation relative to a situation with a single barrier, a process we call 'negative coupling'. More specifically, in our model, negative coupling results either from sexual selection that reduces divergence at all loci, or from reduced LD that occurs because the presence of many females with “mismatched” preferences causes the mating success of recombinant males to become high. Interestingly, the latter effect may even cause LD among preference loci to become negative when recombination rates among loci are low. We conclude that coincident reproductive barriers may not necessarily reinforce each other, and that the underlying loci may not necessarily develop a positive association.

INTRODUCTION

How new species arise is one of the most fundamental questions in evolutionary biology. Speciation relies on the evolution of reproductive isolation between diverging populations and lineages. This process can be mediated by a variety of reproductive barriers, which may often act concurrently. In this case, it is of particular interest to study how different reproductive barriers interact, because theoretically, this interaction may either enhance or reduce overall reproductive isolation. The term *coupling* has been used to refer to the former situation, in which different barriers act in concert, resulting in higher overall reproductive isolation (Butlin and Smadja 2018). Although there are multiple definitions of coupling in the literature (Dopman et al., this volume), this is the definition we adopt here.

Coupling may also be considered from a genetic perspective, as a process governing the establishment and maintenance of linkage disequilibrium (LD; the plural 'linkage disequilibria' will be referred to here as LDs) among loci involved in reproductive isolation. Theoretical studies of coupling have either considered LD between pairs of loci or as a genome-wide phenomenon (although much of this work does not use the term "coupling", e.g. Felsenstein 1981, Barton 1983, Feder and Nosil 2010, Yeaman et al. 2016, reviewed in Dopman et al., this volume). In these views, the strength of coupling is directly related to the extent of realized LD between barriers; larger LD implies stronger coupling, and vice versa (e.g. Barton and de Cara 2009). Although not all studies evaluate coupling directly in terms of reproductive isolation, the buildup of LD and an increase in reproductive isolation may generally be expected to go hand in hand.

It is well established that LD between loci underlying a single reproductive barrier can have a significant impact on speciation (Felsenstein 1981). In this regard, a key role is played by physical linkage between such loci, since LD is more easily maintained when the recombination rate is low. This is consistent with empirical evidence of linkage between loci involved in prezygotic reproductive barriers. For example, in *Heliconius* butterflies, known for differences in wing color patterns that are involved in both divergent ecological adaptation and assortative mating (so-called "magic traits"; Gavrilets 2004, Servedio et al. 2011), quantitative trait locus mapping places a preference locus close to loci determining wing color and pattern (Kronforst et al. 2006, Rossi et al. 2020). In aphids, genes controlling performance on different host plants map to the same genomic regions as genes encoding

assortative mating (Hawthorne and Via 2001), and in the plant *Silene,* genes associated with ecological divergence and those associated with assortative mating were found on the same linkage group (Liu and Karrenberg 2018).

For single prezygotic barriers, the establishment of LD between the underlying loci (e.g. between preference and signal loci) has been studied both theoretically (Servedio and Bürger 2014, 2018) and empirically (Hench et al. 2019). Much less is known about the establishment of LD between loci involved in different prezygotic barriers, although limited empirical evidence suggests that such cross-barrier LD may play a critical role in facilitating speciation. For example, in the Hawaiian cricket genus *Laupala*, which is rich in species that differ in acoustic behavior, speciation has likely been facilitated by assortative mating resulting from tight linkage between multiple trait loci (encoding male song and pulse rate) and the corresponding preference loci (Shaw and Lesnick 2009; Xu and Shaw 2019; Blankers et al. 2019). We might expect such linkage between loci involved in multiple trait/preference sets to be relatively common, as multimodal mating signals (in particular, combinations of acoustic and visual signals) are taxonomically widespread (Halfwerk et al. 2019).

In spite of these putative empirical examples, we have little theoretical understanding of how different sets of mate preference and trait loci may interact, develop LD and influence overall levels of prezygotic isolation (but see Barton and de Cara 2009 for the case of incompatibilities, though these authors did not explicitly consider sexual selection). Here, we address this question using a minimal model with two sets of preference and corresponding mating trait loci. For instance, in the case of the fictional beetle shown in figure 1, we consider two trait loci — encoding color and size —, as well as two associated preference loci — encoding color-based and size-based female preference, respectively. This genetic setting allows us to dissect the buildup of LD and overall reproductive isolation across a continuum of recombination rates between the two preference loci and between the two mating trait loci. In particular, we ask under what conditions the effect of one premating barrier is enhanced by the presence of another such barrier, and whether low recombination between underlying loci necessarily favors such an outcome. In the case of the fictitious beetle in figure 1, we thus ask under what conditions size-based female preference can reinforce the reproductive isolation caused by color-based female preference. For simplicity, we focus on a model of secondary contact between populations in distinct environments (i.e., a two-deme model). Moreover, we assume that the mating traits are also under ecologically divergent selection

(e.g., such that small orange beetles are selectively favored in population 1 and large red ones in population 2; fig. 1); these traits are therefore “magic traits” (Gavrilets 2004). This assumption is necessary, because it has been shown in previous work that, if mating traits are ecologically neutral, divergence in the presence of gene flow cannot be maintained across populations by sexual selection alone (Servedio and Bürger 2014).

Indeed, even when mating traits are under divergent ecological selection, the sexual selection exerted on these traits by the corresponding female preferences can have unintuitive effects (Servedio and Bürger 2014). In particular, when preferences are not themselves under divergent ecological selection, they can maintain different frequencies across populations only through indirect selection, which is mediated by their statistical associations (i.e., LD) with the mating traits. Because these statistical associations are imperfect, indirect divergent selection on the preferences is weaker than the direct ecological and sexual selection that is acting on the mating traits themselves. Preferences will, therefore, maintain less divergent frequencies across populations than will mating traits, meaning that, in each local population, there will be more females with “foreign” preferences than males with “foreign” traits. When preferences are weak, ecologically divergent selection prevails, and mating traits will show strong divergence. But when preferences are strong, sexual selection prevails, which will cause the mating-trait frequencies to mimic the less-divergent preference frequencies. In other words, strong sexual selection homogenizes allele frequencies and trait distributions across populations, because divergence at preference loci is lower than at trait loci.

Stronger preferences thus tend to lead to less divergence, both in models with single loci controlling preferences and traits (Servedio and Bürger 2014) and in quantitative genetic models with similar assumptions (Lande 1982). Given this expectation for a single pair of preference and trait loci (underlying a single reproductive barrier), it is unclear what to expect from the interaction of sets of such loci. One possibility is that the addition of a second set of preference and trait loci effectively reduces gene flow, allowing increased divergence at the first set. Alternatively, introducing a second set of loci could reduce divergence, either by strengthening the homogenizing effect of sexual selection described above, or by another mechanism that is yet undescribed.

METHODS

The model

We consider a two-island population genetics model of haploids with non-overlapping generations. There are four autosomal diallelic loci, two coding for mating traits, T^A and T^B, and two coding for mate preferences, P^A and P^B (as schematized in fig. 1a). Superscripts A and B here refer to the two sets of preference/trait loci that can independently contribute to assortative mating.

The trait loci are subject to divergent viability selection in males (i.e., are "magic traits", Gavrilets 2004; as have been found in nature, Servedio et al. 2011), such that alleles T_k^{A} and T_k^{B} are locally advantageous in population *k* (where *k* = 1 or 2) (fig. 1c). Females with allele P_k^{A} (resp. with allele P_k^{B}) prefer to mate with males with the trait allele T_k^{A} (resp. allele T_k^{B}), regardless of which population they are in at the time (fig. 1b). We assume that alleles P_k^{A} and P_k^{B} are initially predominant in population *k*, generating divergent sexual selection at the T^A and T^B loci. There are thus 16 genotypes, $P_1^{\mathrm{A}}P_1^{\mathrm{B}}T_1^{\mathrm{A}}T_1^{\mathrm{B}}$, $P_1^{\mathrm{A}}P_1^{\mathrm{B}}T_1^{\mathrm{A}}T_2^{\mathrm{B}}$, $P_1^{\mathrm{A}}P_1^{\mathrm{B}}T_2^{\mathrm{A}}T_1^{\mathrm{B}}$, $P_1^{\mathrm{A}}P_1^{\mathrm{B}}T_2^{\mathrm{A}}T_2^{\mathrm{B}}$, through $P_2^{\mathrm{A}}P_2^{\mathrm{B}}T_2^{\mathrm{A}}T_2^{\mathrm{B}}$, the frequencies of which are denoted by $x_{1,k}$ through $x_{16,k}$ respectively, where the second subscript *k* again denotes the population. In the following, we will specifically focus on the alleles P_2^{A}, P_2^{B}, T_2^{A} and T_2^{B}, whose frequencies in population *k* will be denoted by $p_{2,k}^{\mathrm{A}}$, $p_{2,k}^{\mathrm{B}}$, $t_{2,k}^{\mathrm{A}}$ and $t_{2,k}^{\mathrm{B}}$.

The life cycle consists of migration, viability selection, mating, and the production of zygotes, without genetic drift. After migration, the genotypic frequencies are $x_{i,k}^{*} = (1 - m_k)x_{i,k} + m_k x_{i,l}$, where $l = 2$ when $k = 1$ and $l = 1$ when $k = 2$. Parameter m_k denotes the proportion of the population *k* that consists of migrants after migration has occurred (backwards migration rate). Unless stated otherwise, we assume symmetric migration such that $m_1 = m_2 = m$.

Males with alleles T_k^{A} (resp. T_k^{B}) have a selective advantage due to local adaptation, with relative fitness $1 + s_k^{\mathrm{A}}$ (resp. $1 + s_k^{\mathrm{B}}$) in population *k*. After viability selection, the genotypic frequencies in males are:

$$x_{i,k}^{**} = \frac{\left(1+\delta_{i,k}^{\mathrm{A}} s_k^{\mathrm{A}}\right)\left(1+\delta_{i,k}^{\mathrm{B}} s_k^{\mathrm{B}}\right) x_{i,k}^{*}}{\lambda_k}, \qquad [1]$$

where

$$\lambda_k = \sum_{z=1}^{16} \left(1 + \delta_{z,k}^{\mathrm{A}} s_k^{\mathrm{A}}\right)\left(1 + \delta_{z,k}^{\mathrm{B}} s_k^{\mathrm{B}}\right) x_{z,k}^{*}. \qquad [2]$$

Here, $\delta_{i,k}^{\mathrm{A}} = 1$ if genotype *i* has allele T_k^{A} and $\delta_{i,k}^{\mathrm{A}} = 0$ otherwise. Likewise, $\delta_{i,k}^{\mathrm{B}} = 1$ if genotype *i* has allele T_k^{B} and $\delta_{i,k}^{\mathrm{B}} = 0$ otherwise. Unless stated otherwise, we consider symmetric viability selection and the same strength of selection on both loci T^{A} and T^{B}, such that $s_1^{\mathrm{A}} = s_2^{\mathrm{A}} = s_1^{\mathrm{B}} = s_2^{\mathrm{B}} = s$.

Nonrandom mating occurs following preference-trait rules (Kopp et al. 2018). In population *k*, females carrying allele P_1^{A} (resp. P_2^{A}, P_1^{B}, and P_2^{B}) are $1 + \alpha_k^{\mathrm{A},1}$ (resp. $1 + \alpha_k^{\mathrm{A},2}$, $1 + \alpha_k^{\mathrm{B},1}$, and $1 + \alpha_k^{\mathrm{B},2}$) times as likely to mate with a T_1^{A} male (resp. a T_2^{A}, T_1^{B}, and T_2^{B} male) than with a male of the opposite allele, upon encounter. In population *k*, the frequency of mated pairs of females with genotype *i* and males with genotype *j* is thus:

$$M_{i,j,k} = \frac{\left(1+\gamma_{i,j}^{\mathrm{A},1}\alpha_k^{A,1}\right)\left(1+\gamma_{i,j}^{\mathrm{A},2}\alpha_k^{A,2}\right)\left(1+\gamma_{i,j}^{\mathrm{B},1}\alpha_k^{\mathrm{B},1}\right)\left(1+\gamma_{i,j}^{\mathrm{B},2}\alpha_k^{\mathrm{B},2}\right) x_{i,k}^{*} x_{j,k}^{**}}{\Theta_{i,k}}, \qquad [3]$$

where

$$\Theta_{i,k} = \sum_{z=1}^{16} \left(1 + \gamma_{i,z}^{\mathrm{A},1}\alpha_k^{A,1}\right)\left(1 + \gamma_{i,z}^{\mathrm{A},2}\alpha_k^{A,2}\right)\left(1 + \gamma_{i,z}^{\mathrm{B},1}\alpha_k^{\mathrm{B},1}\right)\left(1 + \gamma_{i,z}^{\mathrm{B},2}\alpha_k^{\mathrm{B},2}\right) x_{z,k}^{**}. \qquad [4]$$

Here, $\gamma_{i,j}^{\mathrm{A},1} = 1$ (resp. $\gamma_{i,j}^{\mathrm{A},2} = 1$) if the female genotype *i* carries allele P_1^{A} (resp. P_2^{A}) at the preference locus P^{A} and the male genotype *j* carries allele T_1^{A} (resp. T_2^{A}) at the trait locus T^{A}, and $\gamma_{i,j}^{\mathrm{A},1} = 0$ (resp. $\gamma_{i,j}^{\mathrm{A},2} = 0$) otherwise. The values of $\gamma_{i,j}^{\mathrm{B},1}$ and $\gamma_{i,j}^{\mathrm{B},2}$ are defined analogously on the basis of allele matching between the P^{B} locus in females and the T^{B} locus in males. The normalization in the denominator ensures that all females have equal mating success (meaning that sexual selection acts only on males). We assume symmetrical preference strengths such that $\alpha_k^{\mathrm{A},1} = \alpha_k^{\mathrm{A},2} = \alpha_k^{\mathrm{A}}$ and $\alpha_k^{\mathrm{B},1} = \alpha_k^{\mathrm{B},2} = \alpha_k^{\mathrm{B}}$. Additionally, unless stated otherwise, we assume that mating preference strengths are the same in the two populations, such that $\alpha_1^{\mathrm{A}} = \alpha_2^{\mathrm{A}} = \alpha^{\mathrm{A}}$ and $\alpha_1^{\mathrm{B}} = \alpha_2^{\mathrm{B}} = \alpha^{\mathrm{B}}$.

Mating between haploids leads to the formation of diploid zygotes, which then undergo meiosis and recombination to produce the next generation of haploids. To assess the effect of recombination on trait and preference divergence, we assume that preference loci may be physically linked with each other, with recombination rate r_P between loci P^{A} and P^{B}.

Likewise, we assume that trait loci may be physically linked with each other, with recombination rate r_T between loci T^A and T^B. For simplicity, however, we assume that the preference loci are not physically linked to the mating trait loci (e.g. preference and trait loci are located on different chromosomes). In a supplementary analysis, we relax this assumption and consider that there is physical linkage between all loci, so that the gene order is $P^BP^AT^AT^B$. In another supplementary analysis, we consider $P^AT^AT^BP^B$ as an alternative gene order.

Simulation experiments

We assume secondary contact (a situation that is often found in nature; Harrison 1993), where population 2 is initially fixed for the $P_2^{\mathrm{A}}P_2^{\mathrm{B}}T_2^{\mathrm{A}}T_2^{\mathrm{B}}$ genotype, whereas population 1 has the $P_1^{\mathrm{A}}P_1^{\mathrm{B}}T_1^{\mathrm{A}}T_1^{\mathrm{B}}$ genotype present at a high frequency (= 0.95, to avoid strictly symmetrical starting conditions), with all other genotypes present according to their frequencies at linkage equilibrium.

To assess the long-term equilibrium of the system (e.g. for local allele frequencies and LDs), we run numerical iterations until the change in each allelic frequency is less than 10^{-6} per generation. We report normalized LDs spanning the range $[-1, +1]$. For instance, LD between P^A and T^B in population k is normalized relative to $\min\{p_{2,k}^A(1-t_{2,k}^B), (1-p_{2,k}^A)t_{2,k}^B\}$ when it is positive, and relative to $\min\{p_{2,k}^A t_{2,k}^B, (1-p_{2,k}^A)(1-t_{2,k}^B)\}$ when it is negative (Lewontin, 1964). LDs referred to in the text are always measured within each population, as opposed to across both populations.

To understand the effect of a second set B of preferences and traits on divergence at an "original" set A, we performed comparative simulations with the effect of the preference locus P^B turned off (hereafter called simulation 'without P^B', where $\alpha^A = \alpha$ and $\alpha^B = 0$) or turned on (hereafter called simulations 'with P^B' where $\alpha^A = \alpha^B = \alpha$), the latter representing the presence of a second potential reproductive barrier. Note that, in the simulations without P^B, we nevertheless included the T^B locus (alongside T^A and P^A), to keep the strength of divergent ecological selection the same in both sets of simulations.

Reproductive isolation

To assess the effect of two sets of preferences and traits (sets A and B) on reproductive isolation relative to that with only one "original" set (set A), we numerically estimate the strength of the overall barrier to gene flow at a neutral locus unlinked to all preference and trait loci (Bengtsson, 1985; Barton and Bengtsson, 1986; Westram et al., 2022). To do so, we calculate the effective migration rate, which is inversely proportional to the total strength of barriers to gene flow, from the rate of convergence to equilibrium at the neutral locus (Akerman and Bürger, 2014). More precisely, we consider an additional autosomal diallelic locus N that is neutral and unlinked to all other loci. Starting from the equilibrium state at all other loci, we assume there is initially complete divergence at the neutral locus between populations (with alleles N_1 and N_2 fixed in population 1 and 2, respectively). We then average, over 1,000 generations, the change in allele frequency at the neutral locus relative to the current divergence in allele frequency between populations at this locus. This metric corresponds to the rate of convergence to equilibrium (characterized by an allelic frequency of 0.5 in both populations), and thus corresponds to the effective migration rate, m_{eff}, which is inversely proportional to reproductive isolation, that is, to the strength of the overall barrier to gene flow. We thus define as a measure of reproductive isolation $RI = 1 - \frac{m_{\mathrm{eff}}}{m}$ (Barton and Bengtsson, 1986; Westram et al., 2022). Note that gene flow at neutral loci that are physically linked to divergent loci will be lower than that at the unlinked neutral locus considered here (Barton and Bengtsson 1986; Westram et al. 2022).

RESULTS

Overview of the key results

Although our population genetics model is as simple as possible — with each premating isolating barrier encoded by just two diallelic loci (as schematized in fig. 1) —, contrasting and complex outcomes emerge depending on the recombination rates among loci. In the following sections, we exhaustively describe six qualitatively different regimes. For the convenience of the reader, here we present the key results that we feel are most worth noting.

More importantly, our model shows that reproductive isolation can *decrease* following the coincidence of distinct reproductive barriers (a situation we refer to as 'negative coupling'). Indeed, the presence of a second set of preference and trait loci (encoding an additional premating isolating barrier; see equilibrium state in fig. 2) can, under some conditions, lead to decreased divergence at the first set of loci (encoding an original premating isolating barrier) and to reduced LD between the male trait loci (figs. 3 and 4). This may induce a decrease in the strength of reproductive isolation (fig. 5).

This result can primarily be attributed to two effects. First, the homogenizing effect of sexual selection on allelic divergence (described in the introduction; as shown in a two-locus model in Servedio and Bürger, 2014) can be reinforced when there are two sets of preferences and traits. Second, under some combinations of recombination rates (with higher recombination between preference loci than between trait loci), there can be more recombinant females with mismatched preferences than recombinant males with mismatched traits. The presence of these recombinant females will then generate high mating success for these recombinant males, creating a feedback whereby LD is reduced among both preference and trait loci, and may even become negative. The combinations of these and other effects, described in more detail below, show that it is incorrect to assume that coincident sets of premating barriers will necessarily lead to 'positive coupling' (i.e., an increase in overall reproductive isolation); negative coupling can result instead.

A second set of preference and trait loci impacts divergence according to six different regimes

We first describe how an additional preference locus P^B affects divergence both at the trait locus T^B (due to sexual selection induced by P^B), and at loci P^A and T^A, which form the "original" set of preference and trait loci. Recall that both T^A and T^B are "magic traits" that are also under ecologically divergent selection.

While divergence is generally maintained at all loci in the presence of P^B (fig. 2), it is not necessarily higher than when P^B is absent (fig. 3). First of all, the presence of P^B reduces divergence at the trait locus T^B (figs. 3c and 4; for an exception, see fig. S1 in Supplementary Material), which occurs due to the homogenizing effect of sexual selection described in the introduction (Servedio and Bürger, 2014). By contrast, the impact of P^B on divergence at the

"original" set of preference and trait loci, P^A and T^A, depends on the recombination rates between the preference loci (r_P) and between the trait loci (r_T), and results from the interplay of multiple evolutionary forces. In this subsection, we focus on describing the evolutionary forces that dominate under a variety of regimes that depend on the combination of parameters (r_P, r_T). Note that, although figs. 2, 3, and 5 focus on a single choosiness value ($\alpha = 5$), corresponding to moderately strong preferences, the impact of P^B on divergence at the P^A and T^A loci depends greatly on the level of choosiness (fig. 4).

Overall, figures 2 and 3 allow us to distinguish six different regimes, indicated by Roman numerals in the figures and in the last column of table 1. The six regimes depend on five primary effects of the presence of P^B, which are given in the first column of table 1 (note that regimes **IIIa** and **IIIb** depend on the same primary effect).

In regime **I** (low r_P and high r_T), the presence of the preference locus P^B leads to increased divergence at both the T^A and P^A loci (fig. 3a-b). This is because the presence of P^B increases LD between these loci (figs. 3d and 4a; primary effect (1) in tab. 1). Indeed, there is positive LD both between T^A and T^B (fig. 2g; due to sexual selection induced by $P_1^A P_1^B$ and $P_2^A P_2^B$ females) and between P^A and P^B (fig. 2h; as explained in Box 1). These positive LDs imply that P_1^A females (resp. P_2^A females) are more likely to mate with T_1^A males (resp. T_2^A males) when P^B is present. Increased LD between P^A and T^A, in turn, favors the maintenance of high divergence at the P^A locus through stronger indirect divergent selection on P^A. This thereby reduces the homogenizing effect of sexual selection induced by P^A on T^A, increasing divergence at the T^A locus as well.

In regime **II** (low r_P and lower r_T than in regime **I**), the presence of P^B still increases divergence at the P^A locus, but decreases divergence at the T^A locus (fig. 3a-b and 4b). Strong LD is again maintained both between the trait loci (fig. 2g) and between the preference loci (fig. 2h). In this case, though, these strong LDs increase the maximum level of non-random mating and therefore the strength of homogenizing sexual selection acting on the $T^A T^B$ gene complex (primary effect (2) in tab. 1; through sexual selection acting on the $T_1^A T_1^B$ and $T_2^A T_2^B$ genotypes), which explains why divergence at the T^A locus decreases (fig. 3a). The key difference with regime **I** is that, in regime **II**, r_T is lower and LD between the trait loci is thus higher (darker red in fig. 2g; with $T_1^A T_1^B$ and $T_2^A T_2^B$ genotypes in high

frequency); therefore, homogenizing sexual selection acts more effectively on the T^AT^B gene complex. At the same time, however, the presence of P^B actually increases divergence at the P^A locus (fig. 3b), because the increased LD between P^A and T^A causes stronger indirect divergent selection on P^A (as in regime **I**).

In regimes **IIIa**, **IIIb**, **IV** and **V**, the recombination rate r_T becomes low enough relative to r_P that "recombinant" $T_1^A T_2^B$ and $T_2^A T_1^B$ males become less frequent than "recombinant" $P_1^A P_2^B$ and $P_2^A P_1^B$ females that prefer them, and therefore benefit from high mating success. As explained in Box 1, this effect can decrease LD between the trait loci, and ultimately also between the preference loci. With this background, we can explore the distinction between these four regimes, in which the presence of P^B either decreases divergence at both the T^A and P^A loci (regimes **IIIa**, **IIIb**, and **IV**) or slightly increases divergence at both the T^A and P^A loci (regime **V**).

The hallmark of regimes **IIIa** and **IIIb** (low r_P and low r_T) is negative LD between the preference loci (figs. 2h and 4c-d, primary effect (3) in tab. 1), which arises once sexual selection favoring "recombinant" males lowers the initially positive LD between the trait loci (as explained in Box 1). In turn, this negative LD between the preference loci ultimately generates negative LD between the trait loci T^A and T^B, and also between P^A and T^B due to sexual selection and mate choice (fig. 2f-g; and hatched areas in fig. 3e-f). Through these negative LDs, viability selection on T^B indirectly reduces divergence at both the T^A and P^A loci (fig. 3a-b). This effect is particularly strong in regime **IIIa**, where divergence eventually vanishes at all loci (fig. 2a-d; allele frequencies reach 0.5 in both populations). As a result, in regime **IIIa**, even weak asymmetrical viability selection on T^A or weak asymmetrical preference strength induced by P^A between populations can lead to the loss of genetic variation at the T^A locus (e.g. for $s_1^A = 1.01 s_2^A$ or $\alpha_1^A = 1.01 \alpha_2^A$, respectively; figs. S2 and S3). In regime **IIIb**, this process does not have as strong an effect as in regime **IIIa**, and reduces divergence at all loci without making it vanish.

In regime **IV** (for high r_P and r_T), the presence of P^B decreases divergence at the T^A and P^A loci (fig. 3a-b). LD between all loci remains positive, but the presence of the preference locus P^B decreases LD between loci T^A and T^B (figs. 2g-h, 3f and 4e; primary effect (4) in tab. 1). In

turn, the strength of indirect viability selection on T^A, and consequently also on P^A, is reduced and thus leads to a decrease in divergence at these loci.

Finally, in regime **V** (for high r_P, and low r_T relative to r_P), the presence of P^B very slightly increases divergence at the T^A and P^A loci (fig. 3a-b). The same decrease in LD between loci T^A and T^B occurs as in regime **IV**, but another primary effect prevails: the presence of the preference locus P^B weakens the strength of homogenizing sexual selection on the T^A locus, and hence on the P^A locus indirectly (figs. 3a-b and 4f; primary effect (5) in tab. 1). This effect occurs because homogenizing sexual selection acting on the $T_1^A T_1^B$ and $T_2^A T_2^B$ genotypes is particularly weak (the variation in male mating success is low because $P_1^A P_1^B$ and $P_2^A P_2^B$ females are not overrepresented, as shown in fig. 2h). As a result, divergence at the T^A and P^A loci increases very slightly when P^B is present (fig. 3a-b); this effect is best considered negligible.

We obtain qualitatively the same results when we consider that viability selection on T^A, preference strength induced by P^A, or migration rate is weakly asymmetric between populations (for $s_1^A = 1.01 s_2^A$, $\alpha_1^A = 1.01 \alpha_2^A$ and $m_1 = 1.01 m_2$, respectively; figs. S2-S4), except for the loss of genetic variation in regime **IIIa** mentioned above. Likewise, the same primary effects occur when viability selection is weaker than that implemented in the figures (e.g., for $s = 0.05$ instead of $s = 0.5$; fig. S5), when viability selection acts in both sexes (fig. S6), or when the preference and trait loci are physically linked (with recombination occurring at rate 0.1, instead of free recombination; fig. S1). Note that in simulations where viability selection is weak ($s = 0.01$), we also assumed weak choosiness ($\alpha = 1$), so that frequency-dependent sexual selection does not lead to a loss of allelic divergence (fig. S5); under these conditions, we obtain qualitatively the same results.

A second set of preference and trait loci can decrease reproductive isolation

The way the preference locus P^B influences divergence at the T^A and P^A loci has a notable effect on how P^B affects reproductive isolation, as assessed from the effective migration rate at a neutral unlinked locus (fig. 5). When the presence of P^B increases divergence at both T^A and P^A, reproductive isolation tends to increase, constituting a case of ‘positive coupling’

(traditionally referred to simply as ‘coupling’; Butlin and Smadja 2018). We find, however, that this is the case only in regime **I**, that is, if preference loci are tightly linked but trait loci are essentially unlinked. Even under these conditions, increased divergence at the T^A and P^A loci does not necessarily increase reproductive isolation (as highlighted by the comparison between figs. 3a-b and 5b; this is also the case in regime **V** where divergence at the T^A and P^A loci slightly increases and reproductive isolation is reduced). This is because reproductive isolation can be reduced due to the decrease in divergence at the T^B locus caused by homogenizing sexual selection induced by P^B (fig. 3c).

When, in contrast, the presence of P^B decreases divergence at both the T^A and P^A loci (in regimes **II**, **IIIa**, **IIIb** and **IV**), reproductive isolation can be seen to decrease (fig. 5). We thus, surprisingly, find broad ranges of parameter values for which the coincidence of reproductive barriers reduces overall reproductive isolation. This situation can be referred to as ‘negative coupling’.

DISCUSSION

Our model demonstrates that reproductive isolation can *decrease* following the coincidence of distinct reproductive barriers; this occurs because of (1) the homogenizing effect of sexual selection on allelic divergence and (2) the establishment of particular patterns of LD due to sexual selection, which favor "recombinant" trait combinations. Both of these effects have not been considered previously. We considered a very simple genetic basis underlying two distinct premating reproductive barriers, namely two mating signal loci and their associated preference loci, and showed that the interaction between these loci can, under certain conditions, impede genetic divergence and thus reproductive isolation. We define ‘negative coupling’ as this situation in which different barriers coincide but result in lower overall reproductive isolation (reduced reproductive isolation induced by the second preference locus P^B, as shown in fig. 5b). Note that the parameter space in which negative coupling occurs includes, but is broader than, the parameter space in which LDs are reduced or become negative.

Two evolutionary processes can lead to negative coupling. First, the addition of the second preference locus can strengthen the homogenizing effect of sexual selection, naturally present in this system, that reduces divergence at all loci (primary effect (2) in tab. 1).

Second, sexual selection can reduce the positive LD between the trait loci (primary effects (3) and (4) in tab. 1), which can lead to the establishment of negative LD between preference loci (primary effect (3) in tab. 1; ultimately leading in turn to negative LD between the trait loci). The first evolutionary process is not surprising given that strong nonrandom mating induced by a preference locus has previously been shown to hinder divergence between populations (Servedio and Bürger, 2014). The second process is more unexpected, and arises as a result of hybrids having high mating success due to the high frequency of preference recombinants relative to trait recombinants (because divergence at the preference loci is lower than that at the trait loci). In both cases, the proximate cause of negative coupling is sexual selection. The fact that negative coupling never occurred in the model of Barton and de Cara (2009), is simply due to the fact that sexual selection is not explicitly modeled in their study.

The recombination rates between loci and the strengths of mating preferences determine the outcome of the interaction of loci in terms of divergence and reproductive isolation. Our model shows that negative coupling occurs when the recombination rate between trait loci is low enough relative to that between preference loci, so that trait recombinants are underrepresented relative to preference recombinants. In this case, sexual selection is most effective at favoring (male) trait recombinants and therefore reducing LD between the trait loci, reducing overall reproductive isolation and leading to negative coupling. In addition, when the recombination rate between the preference loci is also low, we show that sexual selection ultimately generates negative LD between the preference loci, which in turn results in negative LD between the trait loci. Altogether, low recombination rates between trait loci and between preference loci promote negative, rather than positive LDs between loci involved in the distinct reproductive barriers.

We expect negative LDs to emerge regardless of the cause of low recombination rate between loci involved in premating isolation. In particular, although we did not explicitly model chromosomal inversions reducing recombination among captured loci (Kirkpatrick, 2010), we predict that the spread of inversions capturing preference loci or their corresponding trait loci should promote the establishment of negative LD, and inhibit local adaptation and speciation. This prediction contrasts with previous theoretical findings that inversions promote premating isolation (in the case of inversions capturing a locus encoding assortative mating and loci with epistatic effects on viability; Trickett and Butlin, 1994, Dagilis

and Kirkpatrick, 2016). The difference between the results of the current study and those of previous studies can be primarily attributed to the fact that the latter have not considered inversions capturing multiple loci involved in 'preference/trait' mating rules, which are known to have unusual effects on divergence (Lande 1982, Servedio and Bürger 2014, Kopp et al. 2018). Our findings should thus provide guidance to interpreting empirical data on the genomics of premating isolation when several barriers are involved (e.g. Ayala et al., 2013, Poelstra et al., 2014). Overall, our results show that tight physical linkage among loci, and more generally low recombination rates, should not be uniformly equated with 'positive coupling' (traditionally called 'coupling'; Butlin and Smadja 2018); in our model, these conditions can instead lead to negative coupling. Counterintuitively, the evolution of tight linkage among preference-trait loci (Schuldiner-Harpaz et al., 2022) may be associated with negative coupling, i.e., with a reduction in the magnitude of reproductive isolation.

To our knowledge, the existence of negative coupling involving loci coding for premating reproductive isolation has not yet been noted in natural systems. Direct evidence of LD among loci involved in premating isolation is scarce, as characterization of the genetic basis of nonrandom mating is still in its infancy (e.g. Poelstra et al., 2014, Merrill et al., 2019, Hench et al. 2019, Enge et al., preprint; but see Ritchie 1992 ; Bakker and Pomiankowski 1995). Furthermore, disentangling positive from negative LD would require characterizing the genetic basis of nonrandom mating not only at the locus level but also at the haplotype level. Nevertheless, indirect evidence of negative coupling could conceivably be explored in natural systems. For example, measurements of phenotypic and allelic clines in natural hybrid zones (e.g. Mallet et al., 1990) could help infer the nature of coupling between loci encoding premating reproductive isolation if there is variation in the strength of nonrandom mating among clines: shallow clines in the presence of strong assortative mating could be due to negative coupling. For comparison purposes, the expected cline widths in the absence of assortative mating can be obtained based on estimates of dispersal and strength of natural selection, i.e., fitness reduction of a parental population in the habitat of the alternative parental population (Bazykin 1969; Mallet et al., 1990; but see Perini et al. 2020). In addition, the nature of coupling that arises among loci encoding premating reproductive isolation can also be inferred from the mating success of hybrids; indeed, our model highlights that high mating success of hybrids can lead to negative coupling. Importantly, this is a frequency-dependent process, with trait recombinants having a high mating success because they are more frequent than preference recombinants. Therefore, the mating success of hybrids

should be measured in natural conditions (e.g. as in Gérard et al., 2006), rather than in mate choice experiments (e.g. as in Chouteau et al., 2017), in order to obtain information on the nature of coupling that may arise.

There is reason to think that the two processes contributing to negative coupling may be dependent on the specifics of the mating system. The homogenizing effect of sexual selection is thought to be dependent to some extent on the underlying preference function. It has been shown to change in some cases with a best-of-n mating system (Servedio and Bürger 2014) and has been hypothesized to vary with open-ended preferences in continuous systems (Servedio and Boughman 2017, based on Lande 1982). Similarly, Servedio and Bürger (2014) found that preferences no longer contribute to homogenize traits across populations when preference strengths are very strong and traits are expressed in both sexes; in preliminary exploration of the case of traits expressed in both sexes we also found that sexual selection induced by the second preference locus P^B does not homogenize populations for high choosiness (in that case, there is no regime **II**). Additionally, the high mating success of rare trait recombinant males, which ultimately leads to low (or in the case of the preference loci, even negative) LDs in the current model, may be buffered if there are search costs and not all preference-recombinant females are able to find their preferred male. Because the factors altering these contributors to negative coupling are to some degree biologically distinct, it is difficult to say to what degree altering any one of them would alter the finding of negative coupling. However, strong search costs have also been found to remove homogenizing sexual selection in some cases in a very similar preference/trait model (Servedio and Bürger 2014), so the effects of search costs would be a promising next front to examine in order to explore the robustness of these effects.

Other assumptions of the model also have the potential to, when altered, produce novel results. Preliminary exploration of alternate orders of the loci in the system indicates that negative coupling can still occur, albeit without LDs becoming negative (e.g., with gene order $P^AT^AT^BP^B$ where we vary within-set recombination rates; fig. S7). Gene order thus conceivably changes the conditions and mechanisms by which negative coupling occurs, but more thorough analyses are needed. Although analytical exploration of the present model could provide interesting insights into the establishment of LD, it is important to note that negative coupling occurs when the recombination rate is particularly low relative to selection, and therefore an analytical exploration using a ‘quasi-linkage equilibrium’ analysis (e.g., as in

Barton and Turelli, 1991) may not allow us to capture the dynamics that we report in this study. In addition, the current model assumes that each independent trait and preference is controlled by a single locus. As many traits are likely to have a polygenic basis, it would be of interest to extend the model in that direction. In that case, LD among loci underlying a given trait, and the resulting indirect selection, would be critical for establishment and maintenance of divergence, and so, in addition to coupling between loci underlying separate traits/preferences, it would be of particular interest to also assess the effect of multiple sets of barriers on the coupling between loci underlying the same trait. Furthermore, it would be interesting to investigate coupling among premating isolating barriers when some loci encode condition-dependent sexual signals, as the evolution at these loci can greatly increase reproductive isolation (van Doorn and Weissing 2004; van Doorn et al. 2009). Finally, another parameter of the model that has a strong influence on the evolutionary dynamics and outcome is preference strength. In this regard, efforts to estimate preference strength from natural populations in a way that connects to this parameter in theoretical models (e.g. Clancey et al. 2021) are worth pursuing.

CONCLUSION

At the onset of this study, we expected the simple result that the addition of a second set of preference and trait loci would strengthen the reproductive isolation established by the first such set. The result of negative coupling, and even more so the fact that it can occur along with the establishment of negative LDs, was surprising to us, and emphasizes that even these simple biological scenarios are complicated and can be difficult to intuit. We hope that this work serves as a cautionary tale, emphasizing that not all coincident barriers will strengthen one another or form positive associations between their underlying loci.

ACKNOWLEDGMENTS

We thank Brian Lerch, Kuangyi Xu, Rebecca Saffran, Åke Brännström, and two anonymous reviewers for comments on the manuscript. This research was supported by grant DEB-1939290 from the National Science Foundation (to MRS) and by grant 2021-05243 from the Swedish Research Council Vetenskapsrådet (to MR).

REFERENCES

Akerman A, Bürger R. 2014. The consequences of gene flow for local adaptation and differentiation: a two-locus two-deme model. *J Math Biol* **68:** 1135-1198.

Ayala D, Guerrero RF, Kirkpatrick M. 2013. Reproductive isolation and local adaptation quantified for a chromosome inversion in a malaria mosquito. *Evolution* **67:** 946-958.

Bakker TCM, Pomiankowski A. 1995. The genetic basis of female mating preferences. *J Evol Biol* **8:** 129-171.

Barton NH. 1983. Multilocus clines. *Evolution* **37:** 454-471.

Barton NH, Bengtsson BO. 1986. The barrier to genetic exchange between hybridising populations. *Heredity* **57:** 357-376.

Barton NH, De Cara MAR. 2009. The evolution of strong reproductive isolation. *Evolution* **63:** 1171-1190.

Barton NH, Turelli M. 1991. Natural and sexual selection on many loci. *Genetics* **127:** 229-255.

Bazykin AD. 1969. Hypothetical mechanism of speciation. *Evolution* **23:** 685-687.

Bengtsson BO. 1985. The flow of genes through a genetic barrier. In *Evolution: Essays in honour of John Maynard Smith* (eds. JJ Greenwood, PH Harvey and M Slatkin), pp. 31-42. Cambridge University Press, Cambridge, MA.

Blankers T, Berdan EL, Hennig RM, Mayer F. 2019. Physical linkage and mate preference generate linkage disequilibrium for behavioral isolation in two parapatric crickets. *Evolution* **73:** 777-791.

Butlin RK, Smadja CM. 2017. Coupling, reinforcement, and speciation. *Am Nat* **191:** 155-172.

Chouteau M, Llaurens V, Piron-Prunier F, Joron M. 2017. Polymorphism at a mimicry supergene maintained by opposing frequency-dependent selection pressures. *Proc Natl Acad Sci USA* **114:** 8325-8329.

Clancey E, Johnson TR, Harmon LJ, Hohenlohe PA. 2022. Estimation of the strength of mate preference from mated pairs observed in the wild. *Evolution*, **76:** 29-41.

Dagilis AJ, Kirkpatrick M. 2016. Prezygotic isolation, mating preferences, and the evolution of chromosomal inversions. *Evolution* **70:** 1465-1472.

Dopman EB, Shaw KL, Servedio MR, Butlin R, Smadja CM. Coupling barriers to gene exchange: Causes and consequences. *Cold Spring Harb Perspect Biol*, this issue (under review).

Enge S, Mérot C, Mozūraitis R, Apšegaitė V, Bernatchez L, Martens GA, Radžiutė S, Pavia H, Berdan EL. preprint. A supergene in seaweed flies modulates male traits and female perception. *BioRxiv* 2021.06.30.450538.

Feder JL, Nosil P. 2010. The efficacy of divergence hitchhiking in generating genomic islands during ecological speciation. *Evolution* **64:** 1729-1747.

Felsenstein J. 1981. Skepticism towards Santa Rosalia, or why are there so few kinds of animals? *Evolution* **35:** 124-138.

Gavrilets S. 2014. Models of speciation: where are we now? *J Hered* **105**: 743-755.

Gérard PR, Klein EK, Austerlitz F, Fernández-Manjarrés JF, Frascaria-Lacoste N. 2006. Assortative mating and differential male mating success in an ash hybrid zone population. *BMC Evol Biol* **6:** 96.

Halfwerk W, Varkevisser J, Simon R, Mendoza E, Scharff C, Riebel K. 2019. Toward testing for multimodal perception of mating signals. *Front Ecol Evol* **7:** 124.

Hawthorne DJ, Via S. 2001. Genetic linkage of ecological specialization and reproductive isolation in pea aphids. *Nature* **412:** 904-907.

Harrison RG. 1993. Hybrid zones and the evolutionary process. Oxford University Press, Oxford.

Hench K, Vargas M, Höppner MP, McMillan WO, Puebla O. 2019. Inter-chromosomal coupling between vision and pigmentation genes during genomic divergence. *Nat Ecol Evol* **3:** 657-667.

Kirkpatrick M. 2010. How and why chromosome inversions evolve. *PLoS Biol* **8:** e1000501.

Kronforst MR, Young LG, Kapan DD, McNeely C, O'Neill RJ, Gilbert LE. 2006. Linkage of butterfly mate preference and wing color preference cue at the genomic location of "wingless". *Proc Natl Acad Sci USA* **103:** 6575-6580.

Kopp M, Servedio MR, Mendelson TC, Safran RJ, Rodríguez RL, Hauber ME, Scordato EC, Symes LB, Balakrishnan CN, Zonana DM, van Doorn GS. 2018. Mechanisms of assortative mating in speciation with gene flow: Connecting theory and empirical research. *Am Nat* **191:** 1-20.

Lande R. 1982. Rapid origin of sexual isolation and character divergence in a cline. *Evolution* **36:** 213-223.

Lewontin RC. 1964. The interaction of selection and linkage. I. General considerations: heterotic models. *Genetics* **49:** 49-67.

Liu X, Karrenberg S. 2018. Genetic architecture of traits associated with reproductive barriers in *Silene*: Coupling, sex chromosomes and variation. *Mol Ecol* **27:** 3889-3904.

Merrill RM, Rastas P, Martin SH, Melo MC, Barker S, Davey J, McMillan WO, Jiggins CD. 2019. Genetic dissection of assortative mating behavior. *PLoS Biol* **17:** e2005902.

Mallet J, Barton N, Lamas G, Santisteban J, Muedas M, Eeley H. 1990. Estimates of selection and gene flow from measures of cline width and linkage disequilibrium in heliconius hybrid zones. *Genetics* **124:** 921-936.

Perini S, Rafajlović M, Westram AM, Johannesson K, Butlin RK. 2020. Assortative mating, sexual selection, and their consequences for gene flow in *Littorina*. *Evolution* **74:** 1482-1497.

Poelstra JW, Vijay N, Bossu CM, Lantz H, Ryll B, Müller I, Baglione V, Unneberg P, Wikelski M, Grabherr MG, Wolf JB. 2014. The genomic landscape underlying phenotypic integrity in the face of gene flow in crows. *Science* **344:** 1410-1414.

Ritchie MG. 1992. Setbacks in the search for mate preference genes. *Trends Ecol Evol* **7:** 328-329.

Rossi M, Hausmann AE, Thurman TJ, Montgomery SH, Papa R, Jiggins CD, McMillan WO, Merrill RM. 2020. Visual mate preference evolution during butterfly speciation is linked to neural processing genes. *Nat Commun* **11:** 4763.

Servedio MR, Boughman JW. 2017. The role of sexual selection in local adaptation and speciation. *Annu Rev Ecol Evol Syst* **48:** 85-109.

Servedio MR, Bürger R. 2014. The counterintuitive role of sexual selection in species maintenance and speciation. *Proc Natl Acad Sci USA* **111:** 8113-8118.

Servedio MR, Bürger R. 2018. The effects on parapatric divergence of linkage between preference and trait loci versus pleiotropy. *Genes* **9:** 217.

Servedio MR, Van Doorn GS, Kopp M, Frame AM, Nosil P. 2011. Magic traits in speciation: 'magic' but not rare? *Trends Ecol Evol* **26:** 389-397.

Shaw KL, Lesnick SC. 2009. Genomic linkage of male song and female acoustic preference QTL underlying a rapid species radiation. *Proc Natl Acad Sci USA* **106:** 9737-9742.

Schuldiner-Harpaz T, Merrill RM, Jiggins CD. 2022. Evolution of physical linkage between loci controlling ecological traits and mating preferences. *J Evol Biol* **35:** 1537-1547.

Trickett AJ, Butlin RK. 1994. Recombination suppressors and the evolution of new species. *Heredity* **73:** 339-345.

van Doorn GS, Edelaar P, Weissing FJ. 2009. On the origin of species by natural and sexual selection. *Science* **326:** 1704-1707.

van Doorn GS, Weissing FJ. 2004. The evolution of female preferences for multiple indicators of quality. *Am Nat* **164:** 173-186.

Westram AM, Stankowski S, Surendranadh P, Barton NH. 2022. What is reproductive isolation? *J Evol Biol* **35:** 1143-1164.

Xu M, Shaw KL. 2019. Genetic coupling of signal and preference facilitates sexual isolation during rapid speciation. *Proc R Soc B* **286:** 20191607.

Yeaman S, Aeschbacher S, Bürger R. 2016. The evolution of genomic islands by increased establishment probability of linked alleles. *Mol Ecol* **25:** 2542-2558.

BOX

Box 1. Establishment of LD between the preference loci.

The impact of a second set of preferences and traits (set B) on divergence at an "original" set of preferences and traits (set A) depends greatly on the LD that builds up between the preference loci, P^A and P^B. As explained in the main text, for some combinations of parameters, the establishment of positive LD between the preference loci increases divergence at the P^A and T^A loci (primary effect (1) in tab. 1, prevailing in regime **I**), while for other combinations of parameters, the establishment of negative LD between the preference loci leads to the opposite outcome (primary effect (3) in tab. 1, prevailing under regimes **IIIa** and **IIIb**). These patterns of LD between the preference loci arise due to the joint action of mate choice (leading to nonrandom pairing of female and male genotypes) and variation in male mating success (sexual selection), as follows.

During nonrandom mating, *mate choice* is based on the match/mismatch between the alleles carried by females at the preference loci and those carried by males at the corresponding trait loci (fig. 1b), leading to positive LD within sets of preference and trait loci (i.e., between P^A and T^A, and between P^B and T^B; fig. 2e). Once this positive LD is established, and because divergent selection and migration jointly generate positive LD between the trait loci T^A and T^B, mate choice also generates positive LD between the P^A and P^B loci. This occurs although the P^B locus is neutral in males; for example, when a P_1^A female chooses a T_1^A male, this male is more likely to carry a P_1^B than a P_2^B allele, due to the LD-chain T^A – T^B – P^B.

In addition to *mate choice*, LD is also influenced by *variation in male mating success*, that is, by sexual selection. Female mate choice determines the mating success of males according to their genotype at the trait loci, and thus changes the LD between these loci. Because there is always positive LD between the preference and trait loci within sets (between P^A and T^A, and between P^B and T^B, due to mate choice as explained above), the effect of sexual selection on the trait loci then feeds back to LD between the preference loci.

Specifically, and critically to explain the negative LD among loci that we often see in this model, sexual selection reduces LD between the trait loci when "recombinant" $T_1^A T_2^B$ and

$T_2^{\mathrm{A}}T_1^{\mathrm{B}}$ males benefit from high mating success, i.e., when they are in lower frequency than "recombinant" $P_1^{\mathrm{A}}P_2^{\mathrm{B}}$ and $P_2^{\mathrm{A}}P_1^{\mathrm{B}}$ females that prefer them. This condition is often met, especially when r_T is low enough relative to r_P, because divergence at the trait loci is higher than divergence at the preference loci, and $T_1^{\mathrm{A}}T_2^{\mathrm{B}}$ and $T_2^{\mathrm{A}}T_1^{\mathrm{B}}$ recombinant males are therefore less frequent than $P_1^{\mathrm{A}}P_2^{\mathrm{B}}$ and $P_2^{\mathrm{A}}P_1^{\mathrm{B}}$ recombinant females. Reduced LD between trait loci then leads to reduced LD between the preference loci, as discussed above. Ultimately, both of these LDs can become negative. However, negative LD more readily occurs between the preference loci than between the trait loci. This is because the above-described decrease in LD due to mate choice is partially counteracted by an increase in LD due to migration and divergent selection across populations, and this latter effect is stronger for trait loci (which are under direct selection) than for preference loci (which are under indirect selection). Examination of time series (not shown) reveals, indeed, that the LD between preference loci becomes negative first, generally followed by negative LD between the trait loci (note that negative LD between the preference loci will cause the mating success of "recombinant" $T_1^{\mathrm{A}}T_2^{\mathrm{B}}$ and $T_2^{\mathrm{A}}T_1^{\mathrm{B}}$ males to increase even more).

On the other hand, when r_T is high enough relative to r_P (in regimes **I** and **II**), "recombinant" $T_1^AT_2^B$ and $T_2^AT_1^B$ males are at higher frequency than $P_1^AP_2^B$ and $P_2^AP_1^B$ females and therefore experience strong competition for females that prefer them. In that case, the mean mating success of $T_1^AT_2^B$ and $T_2^AT_1^B$ males is lower than that of $T_1^AT_1^B$ and $T_2^AT_2^B$ males. In consequence, LD between the trait loci increases due to sexual selection, and so does LD between the preference loci (both of these LDs therefore remain positive).

FIGURES AND TABLE

Figure 1. Schematic of model assumptions with a fictitious beetle used as an illustration. (**a**) In our model, we consider four diallelic loci, two trait loci and the two associated preference loci. For example, here, one trait locus encodes the color and the other trait locus encodes the size of the beetle. In addition, one preference locus encodes the female's mating preference according to the male's color (preference for red-spotted males or for orange males), while the other preference locus encodes the female's mating preference according to the male's size (preference for large-sized males or for small-sized males). (**b**) Hence, during mating, females express a preference for males according to the combination of trait alleles expressed by males; this generates sexual selection on trait loci, the strength of which is reflected in the thickness of the arrows. (**c**) Divergence occurs across two populations, where viability selection favors different genotypes at the trait loci and where migration opposes divergence.

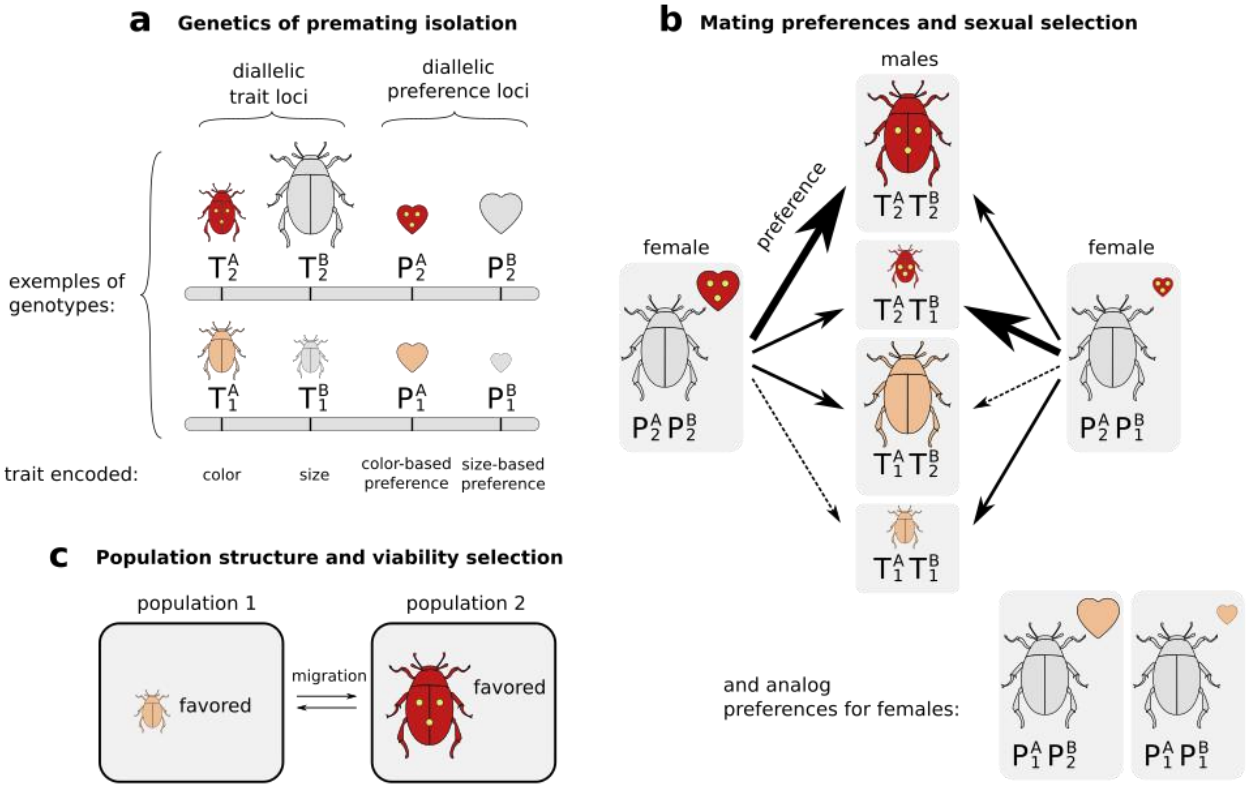

Figure 2. Equilibrium state in simulations with P^B depending on the recombination rates between the preference loci (r_P) and between the trait loci (r_T), focusing on allelic divergence (**a**-**d**) and normalized LD (**e**-**h**). At each locus, allelic divergence is calculated as the absolute difference between the allelic frequencies in each population. Normalized LDs between loci are shown for population 2, but values in population 1 are extremely similar (see fig. 4). Because we assume free recombination between the preference and trait loci, in simulations with P^B, normalized LD between loci P^B and T^A is the same as the one between P^A and T^B, and normalized LD between loci P^B and T^B is the same as the one between P^A and T^A; we thus do not represent these LDs (see annotation in panels **e** and **f**). In panel **a**, Roman numerals refer to the different regimes summarized in tab. 1 for specific recombination rates (as implemented in the different panels of fig. 4). Here, $s = 0.5$, $m = 0.01$ and $\alpha = 5$.

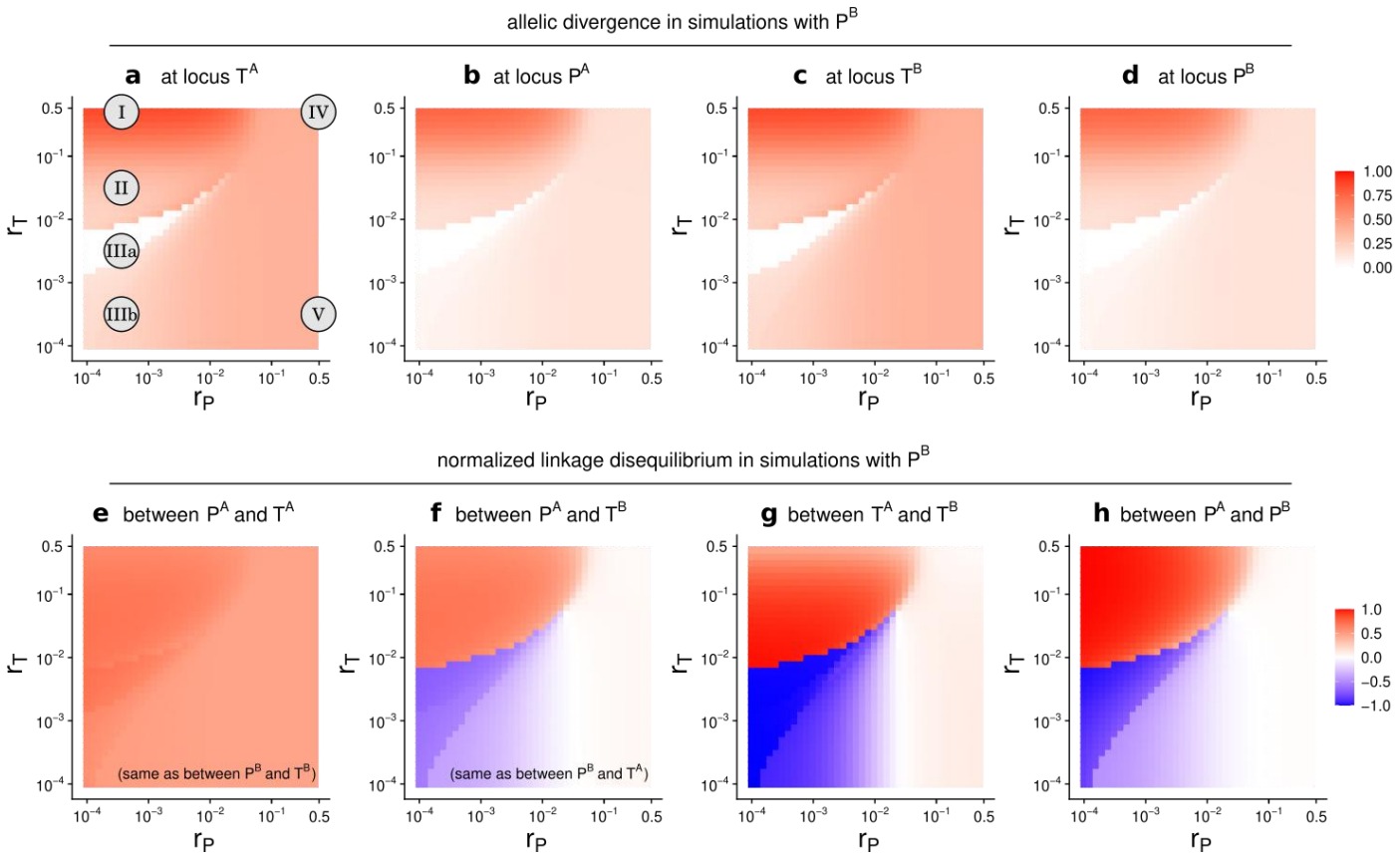

Figure 3. Comparison of equilibrium states with versus without P^B depending on the recombination rates between the preference loci (r_P) and between the trait loci (r_T). We compare the equilibrium states with P^B versus without P^B, and represent the difference in allelic divergence (**a**-**c**) and the difference in normalized LD (**d**-**f**). See caption of fig. 2 for details on these metrics. The hatched area represents the parameter region for which LD is negative in the simulations with P^B (see fig. 2f-g). LD is always positive without P^B (not shown). In panel **a**, Roman numerals refer to the different regimes summarized in tab. 1 for specific recombination rates (as implemented in the different panels of fig. 4). The reduced divergence at the T^A locus in regime **II** and the slight increase at the T^A and P^A loci in regime **V** with P^B versus without P^B may not be visible (**a**). Here, $s = 0.5$, $m = 0.01$ and $\alpha = 5$.

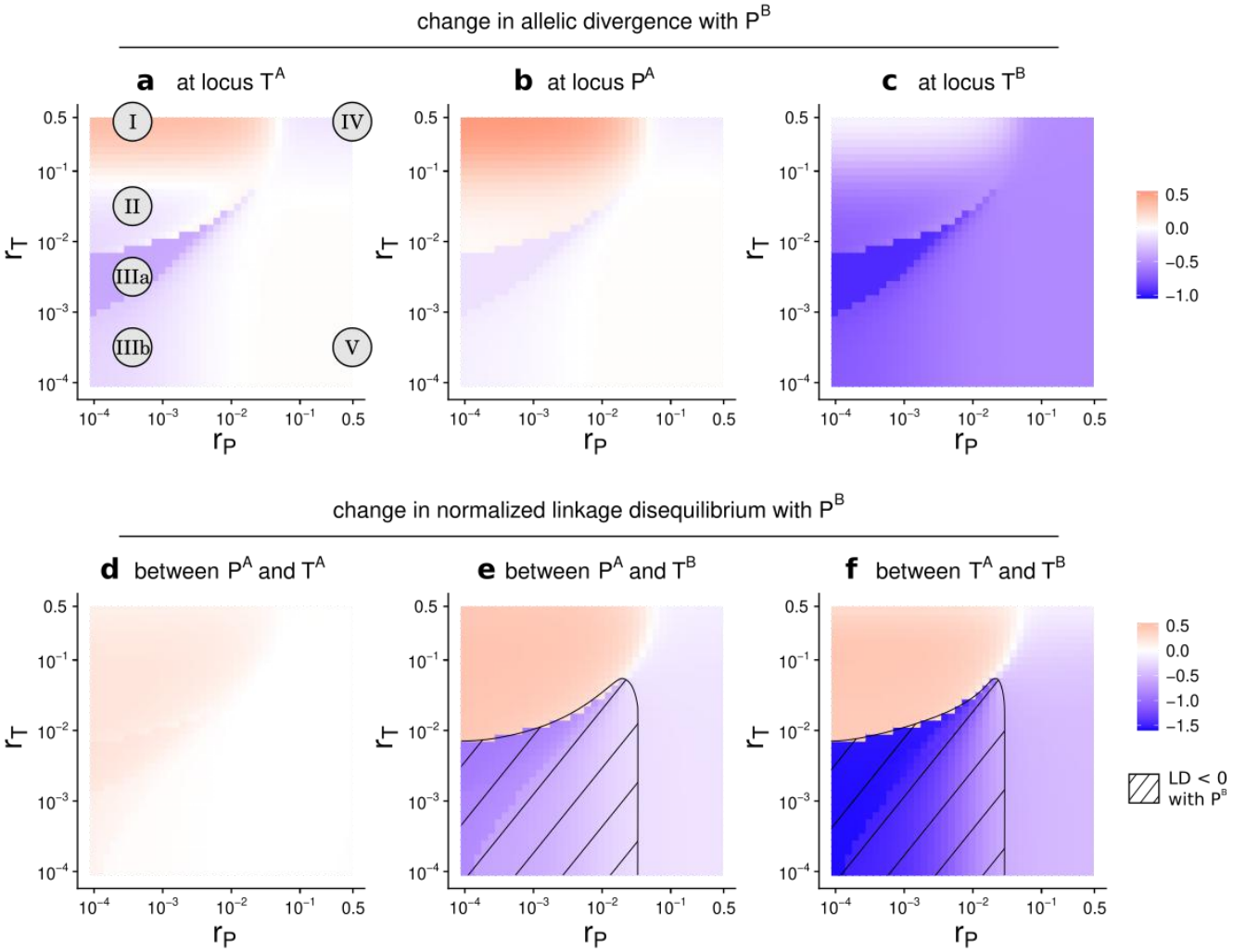

Figure 4. Equilibrium states with or without P^B depending on the recombination rates (r_P and r_T) and on the strength of preference induced by each preference locus (α). We represent allelic frequencies (frequencies of the alleles P_2^A, P_2^B, T_2^A or T_2^B) and normalized LDs in each population (blue for population 1, red for population 2), in simulations with P^B (solid lines) or without P^B (dashed lines). To simplify the representation, we do not show lines where allelic variation is lost at all loci (when allelic frequencies reach 1 due to the asymmetric starting conditions). Note that normalized LDs are the same in both populations, and red and blue lines therefore overlap. Because we assume free recombination between the preference and trait loci, in simulations with P^B, normalized LD between loci P^B and T^A is the same as the one between P^A and T^B, and normalized LD between loci P^B and T^B is the same as the one between P^A and T^A; we thus do not represent these LDs. In each panel, we consider different combinations of recombination rates, r_P and r_T, which correspond to the Roman numerals in the other figures. The vertical gray lines in all panels represent the strength of preference implemented in figs. 2, 3 and 5 ($\alpha = 5$). Close inspection of the simulations allowed us to determine that some asymmetries in the figure (e.g. in panels c and e) are ultimately due to the asymmetries that we set in initial allelic frequencies. Here, $s = 0.5$ and $m = 0.01$.

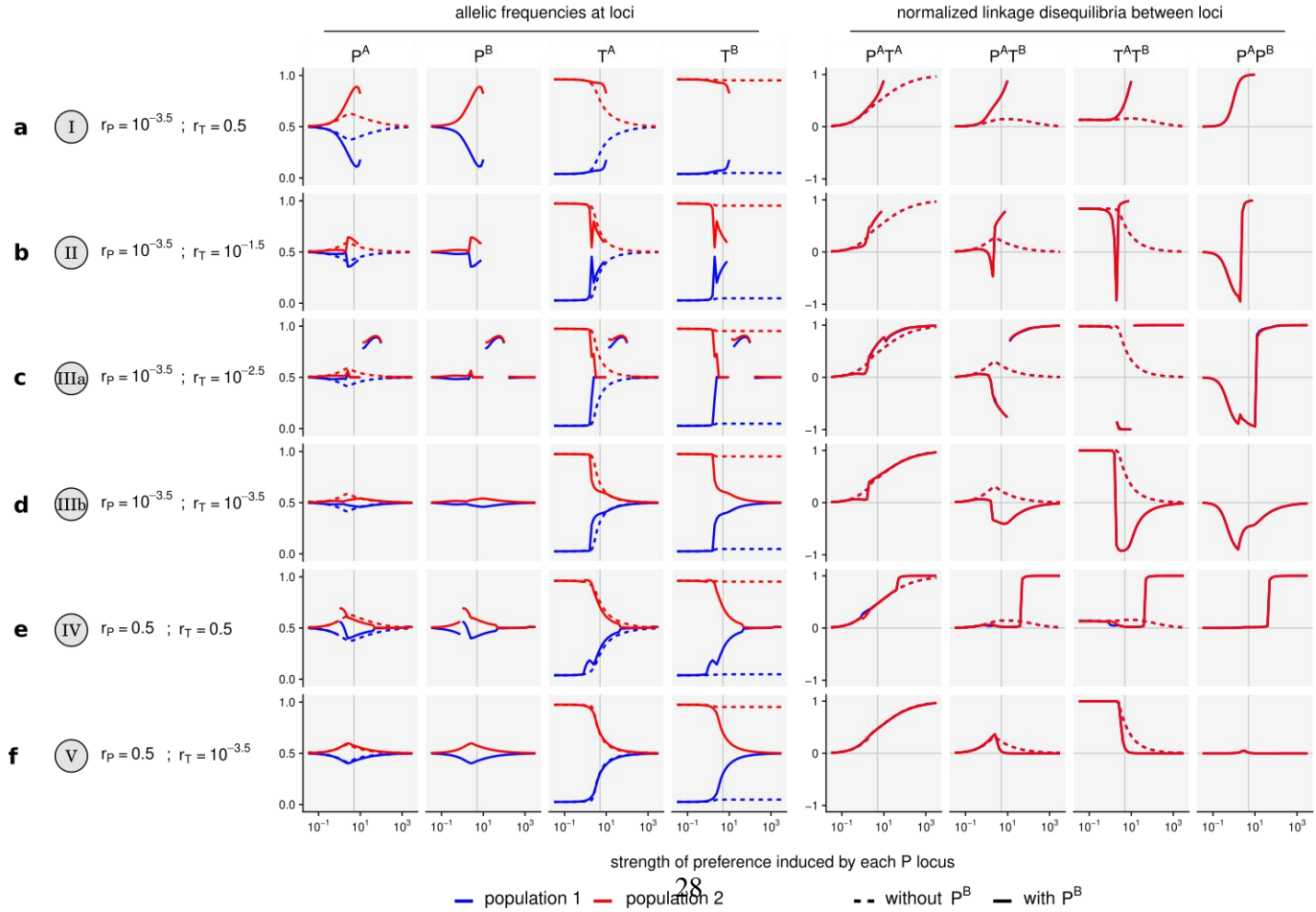

Figure 5. Reproductive isolation (RI) assessed from the effective migration rate at a neutral unlinked locus depending on the recombination rates between the preference loci (r_P) and between the trait loci (r_T). (**a**) Reproductive isolation in simulations with P^B. (**b**) Change in reproductive isolation in simulations with P^B relative to that without P^B. In panel **b**, Roman numerals refer to the different regimes summarized in tab. 1 for specific recombination rates (as implemented in the different panels of fig. 4). Here, $s = 0.5$, $m = 0.01$ and $\alpha = 5$.

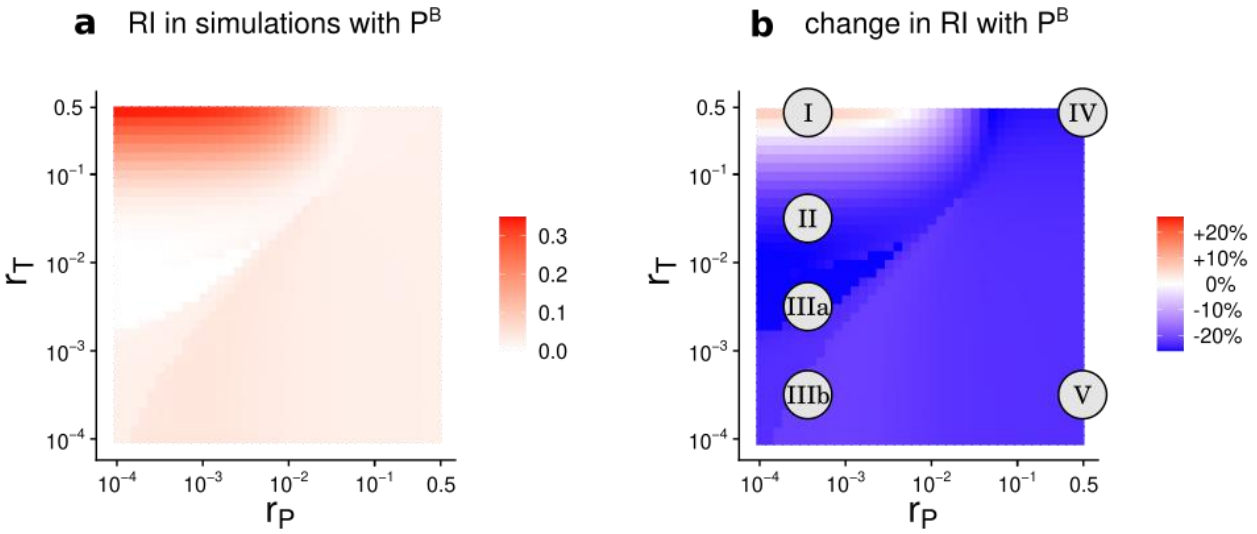

Table 1. Summary of the primary effects of P^B ultimately affecting divergence at the P^A and T^A loci. The regimes referred to in the last column are numbered as on figures 2-5, and correspond to the parameter combinations for which each primary effect prevails.

Primary effect of P^B	**Consequence on divergence at P^A**	**Consequence on divergence at T^A**	**Dependence on recombination rates**	**Regimes**
(1) Increased positive LD between P^A and T^A	increase in divergence via indirect viability selection (through LD between P^A and T^A)	increase in divergence via weaker homogenizing sexual selection (due to the increased divergence at P^A)	when $P_1^A P_1^B$ and $P_2^A P_2^B$ are very frequent relative to $T_1^A T_1^B$ and $T_2^A T_2^B$, for $r_P << r_T$	**I**
(2) Stronger homogenizing sexual selection on the $T^A T^B$ gene complex	increase in divergence via indirect selection (through LD of P^A with T^A and T^B)	decrease in divergence via stronger homogenizing sexual selection	when $P_1^A P_1^B$ and $P_2^A P_2^B$ are frequent relative to $T_1^A T_1^B$ and $T_2^A T_2^B$, for $r_P < r_T$	**II**
(3) Decreased LD between T^A and T^B, leading to the establishment of negative LD between P^A and P^B	decrease in divergence via indirect viability selection (through the establishment of negative LD between P^A and T^B)	decrease in divergence via indirect viability selection (through the establishment of negative LD between T^A and T^B)	when $T_1^A T_2^B$ and $T_2^A T_1^B$ males have a high mating success, which is the case when r_T is low enough relative to r_P, and when negative LD between P^A and P^B is maintained, which is the case when r_P is low	**IIIa - IIIb**
(4) Decreased LD between T^A and T^B, without establishment of negative LD between P^A and P^B	decrease in divergence via indirect viability selection (through decreased LD between P^A and T^B)	decrease in divergence via indirect viability selection (through decreased LD between T^A and T^B)	when $T_1^A T_2^B$ and $T_2^A T_1^B$ males have a high mating success, which is the case when r_T is low enough relative to r_P, and when negative LD between P^A and P^B is not maintained, which is the case when r_P is high.	**IV**
(5) Weaker homogenizing sexual selection on the T^A locus	negligible increase in divergence via indirect selection (through LD of P^A with T^A and T^B)	negligible increase in divergence via weaker homogenizing sexual selection	when $P_1^A P_1^B$ and $P_2^A P_2^B$ females impose weak sexual selection on the $T_1^A T_1^B$ and $T_2^A T_2^B$ genotypes, which is particularly the case when $r_P >> r_T$	**V**

Supplementary Material for:

Negative coupling: the coincidence of premating isolating barriers can reduce reproductive isolation

Thomas G. Aubier, Michael Kopp, Isaac J. Linn, Oscar Puebla,
Marina Rafajlović, Maria R. Servedio

Content:

Figure S1. Comparison of equilibrium states with versus without P^B, with linkage between the preference and the trait loci (with recombination occurring at rate 0.1, assuming that gene order is $P^BP^AT^AT^B$). We compare the equilibrium states with P^B versus without P^B, and represent the change in allelic divergence (**a**-**c**) and the change in normalized LD (**d**-**f**). See caption of fig. 3 for details (but note that the color scale is different here). In panel **a**, Roman numerals refer to the different regimes summarized in tab. 1, but note that they are not placed at the same locations (i.e., the same combinations of r_T and r_P) as in fig. 3 (hence the use of a pink background; see explanation below). Here, green pixels represent parameter combinations where genetic variation is lost at the T^A and T^B loci (loci P^A and P^B then become neutral). We obtain a similar outcome as with free recombination between the preference and the trait loci (fig. 3), except for the loss of genetic variation that occurs in the domain of regime **IIIa**, and the fact that primary effect (1) under regime **I** can occur alongside an increase in divergence at the T^B locus due to the presence of P^B (at the very top left of panel **c**). In particular, we observe that the same regimes, from **I** to **V** under which primary effects (1) to (5) prevail as summarized in tab. 1, occur as in the case of free recombination (fig. 3). Here, $s = 0.5$, $m_2 = 0.01$ and $\alpha = 5$.

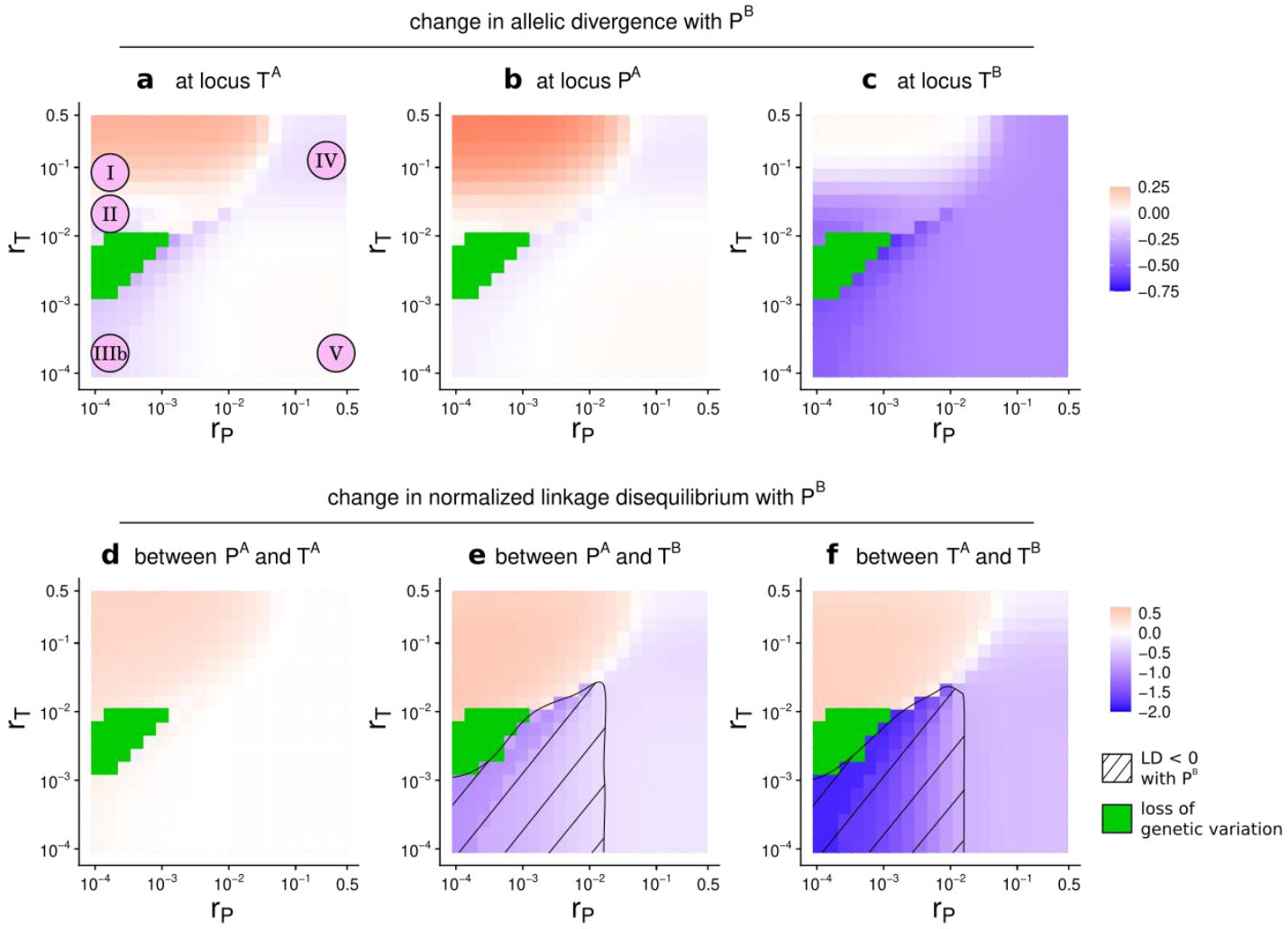

Figure S2. Comparison of equilibrium states with versus without P^B, with weak asymmetrical viability selection on T^A between populations ($s_1^A = 1.01\, s_2^A$). We compare the equilibrium states with P^B versus without P^B, and represent the change in allelic divergence (**a**-**c**) and the change in normalized LD (**d**-**f**). See caption of fig. 3 for details. Here, green pixels represent parameter combinations where genetic variation is lost at the T^A and T^B loci (loci P^A and P^B then become neutral). We obtain qualitatively the same outcome as without asymmetrical viability selection (fig. 3), except for the loss of genetic variation that occurs in the domain of regime **IIIa**. Here, $s_2^A = 0.5$, $m = 0.01$ and $\alpha = 5$.

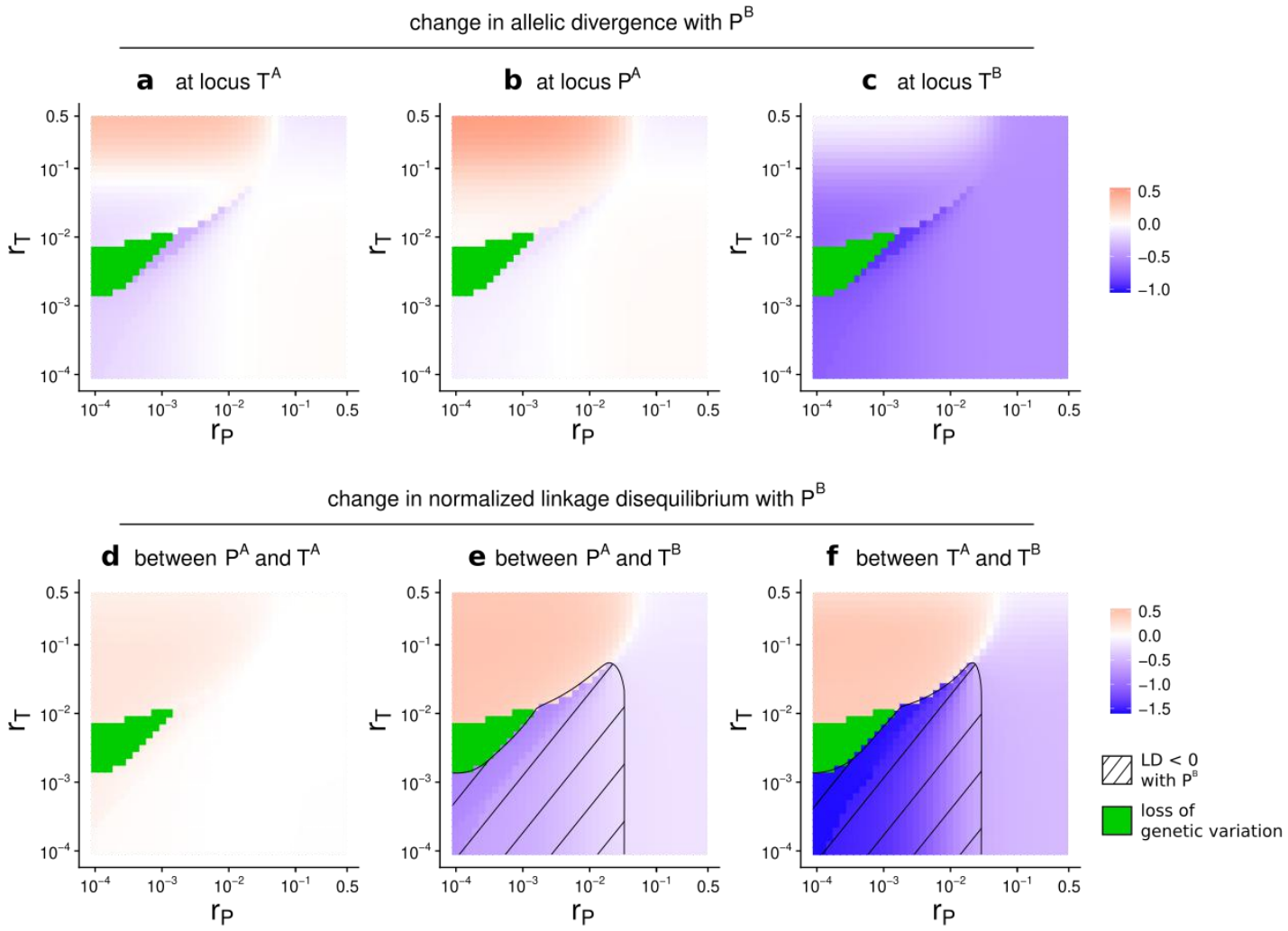

Figure S3. Comparison of equilibrium states with versus without P^B, with weak asymmetrical preference strength induced by P^A between populations ($\alpha_1^A = 1.01\alpha_2^A$). We compare the equilibrium states with P^B versus without P^B, and represent the change in allelic divergence (**a**-**c**) and the change in normalized LD (**d**-**f**). See caption of fig. 3 for details. Here, green pixels represent parameter combinations where genetic variation is lost at the T^A and T^B loci (loci P^A and P^B then become neutral). We obtain qualitatively the same outcome as without asymmetrical preference strength (fig. 3), except for the loss of genetic variation that occurs in the domain of regime **IIIa**. Here, $s = 0.5$, $m = 0.01$ and $\alpha_2^A = 5$.

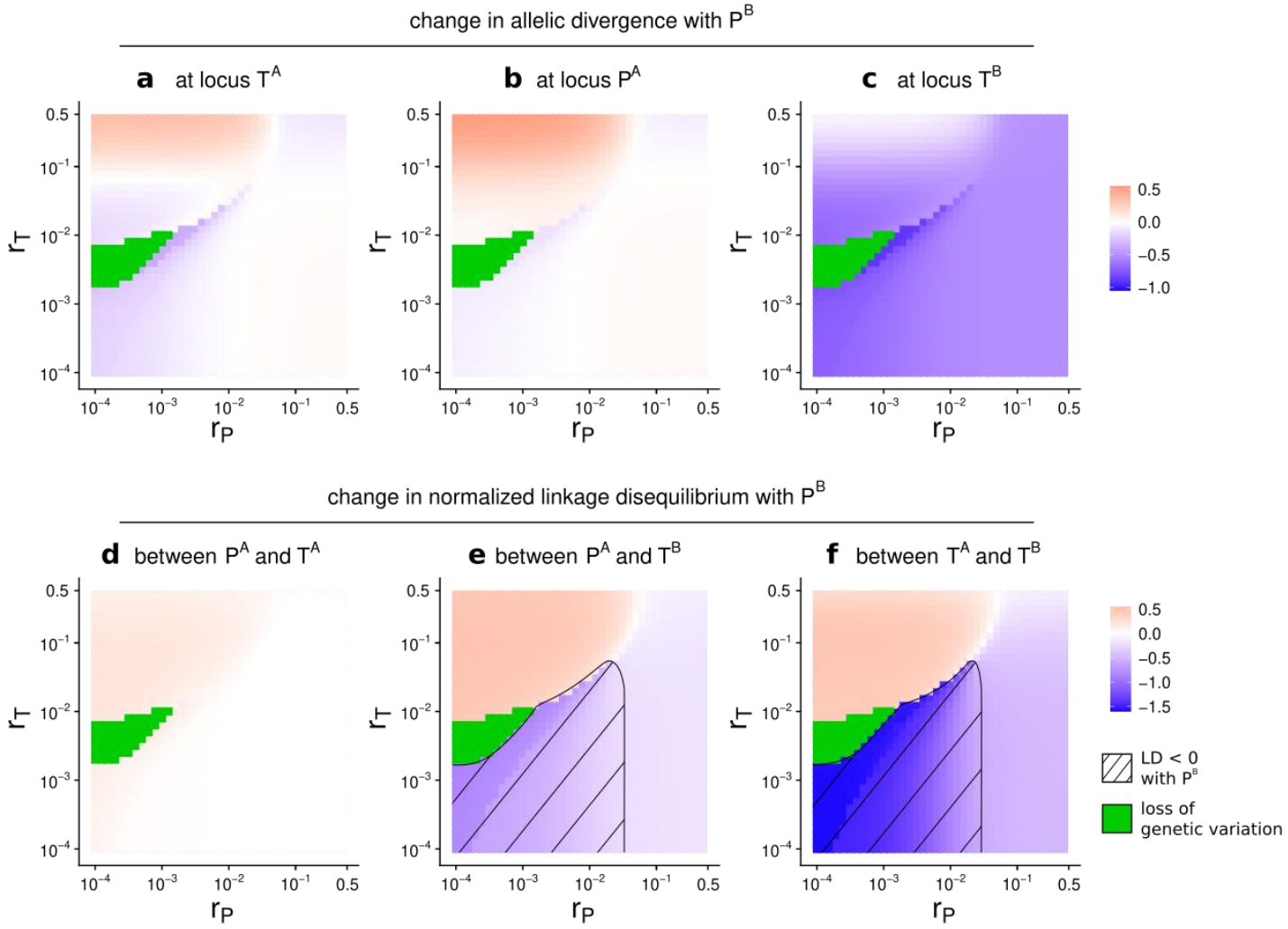

Figure S4. Comparison of equilibrium states with versus without P^B, with weak asymmetrical migration between populations ($m_1 = 1.01m_2$). We compare the equilibrium states with P^B versus without P^B, and represent the change in allelic divergence (**a**-**c**) and the change in normalized LD (**d**-**f**). See caption of fig. 3 for details. We obtain qualitatively the same outcome as without asymmetrical migration (fig. 3). Here, $s = 0.5$, $m_2 = 0.01$ and $\alpha = 5$.

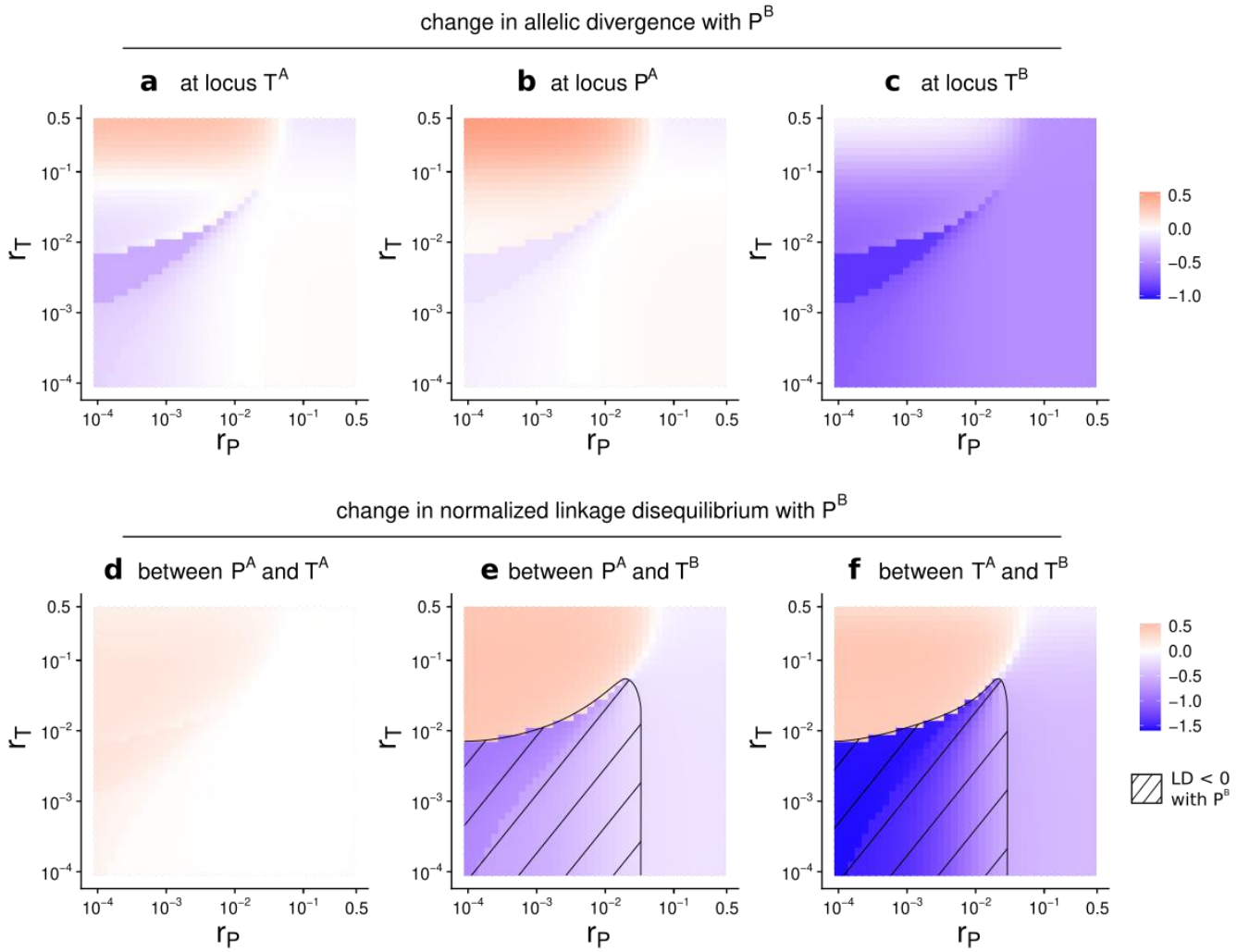

Figure S5. Comparison of equilibrium states with versus without P^B, with weaker viability selection and choosiness ($s = 0.05;\ \alpha = 1$). We compare the equilibrium states with P^B versus without P^B, and represent the change in allelic divergence (**a**-**c**) and the change in normalized LD (**d**-**f**). See caption of fig. 3 for details (but note that the color scale is different here). In panel **a**, Roman numerals refer to the different regimes summarized in tab. 1, but note that they are not placed at the same locations (i.e., the same combinations of r_T and r_P) as in fig. 3 (hence the use of a pink background; see explanation below). Here, green pixels represent parameter combinations where genetic variation is lost at the T^A and T^B loci (loci P^A and P^B then become neutral). We obtain a similar outcome as with strong viability selection and choosiness (fig. 3), except for the loss of genetic variation that occurs here, and the absence of regime **V**. In particular, we observe that the same regimes (from **I** to **IV**) under which primary effects (1) to (4) prevail as summarized in tab. 1, occur as in the case of strong viability selection and choosiness (fig. 3). With such low viability selection ($s = 0.05$) but with stronger choosiness (e.g. $\alpha = 5$), a loss of genetic variation occurs for most recombination rates, due to the homogenizing effect of sexual selection that is not overcome by divergent viability selection (not shown). Here, $m = 0.01$.

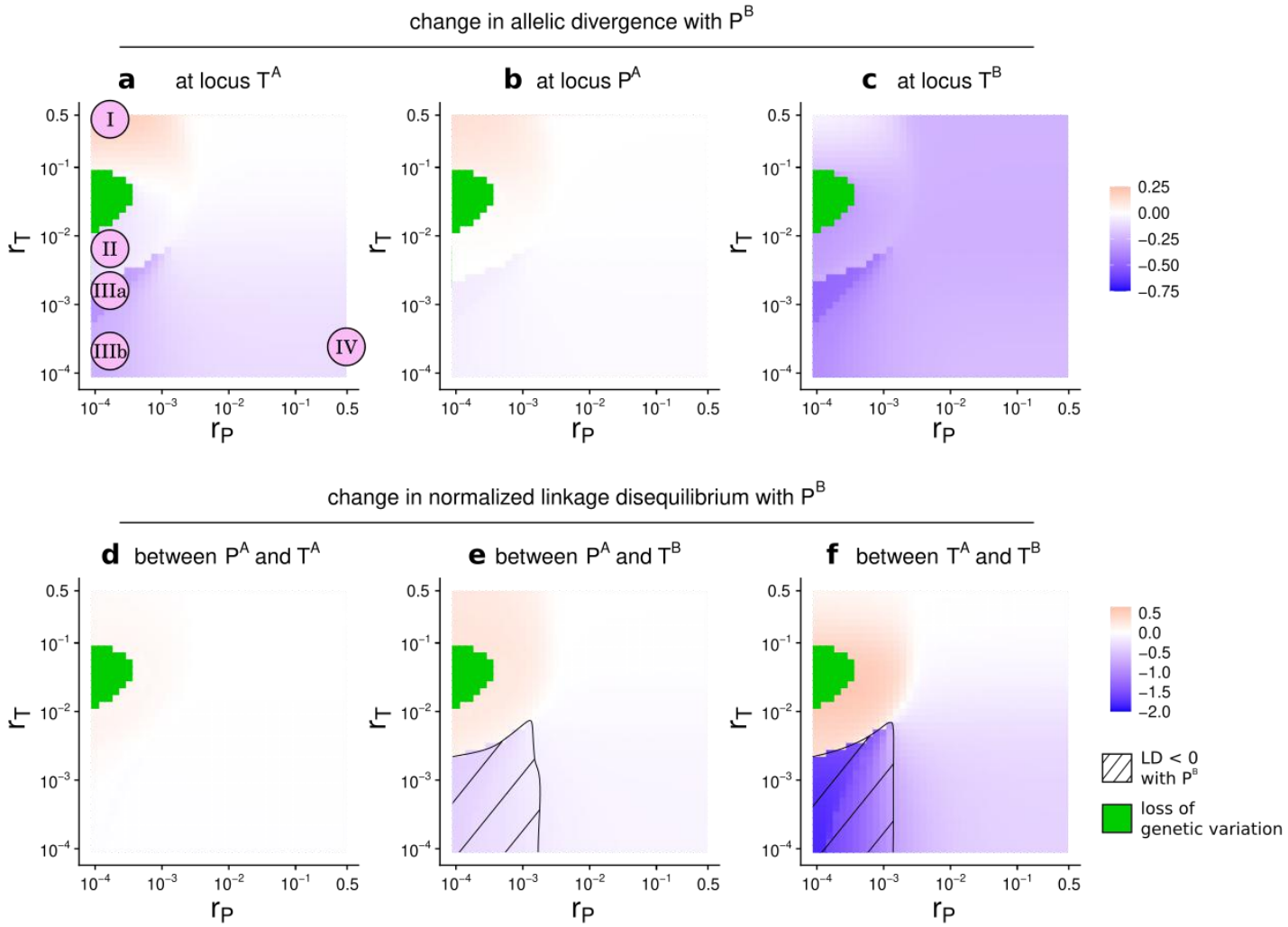

Figure S6. Comparison of equilibrium states with versus without P^B, with viability selection acting in both sexes and with weaker viability selection and choosiness ($s = 0.05;\ \alpha = 1$). We compare the equilibrium states with P^B versus without P^B, and represent the change in allelic divergence (**a**-**c**) and the change in normalized LD (**d**-**f**). See caption of fig. 3 for details (but note that the color scale is different here). In panel **a**, Roman numerals refer to the different regimes summarized in tab. 1, but note that they are not placed at the same locations (i.e., the same combinations of r_T and r_P) as in fig. 3 (hence the use of a pink background; see explanation below). Here, green pixels represent parameter combinations where genetic variation is lost at the T^A and T^B loci (loci P^A and P^B then become neutral). We obtain a similar outcome as with viability selection acting in males only (fig. S5), except for the loss of genetic variation, which occurs for a large set of recombination rates, and for the absence of regime **V**. In particular, we observe that the same regimes, from **I** to **IV** under which primary effects (1) to (4) prevail as summarized in tab. 1, occur as in the case of viability selection acting in males only (fig. S5). With stronger viability selection and choosiness (e.g. $s = 0.5$ and $\alpha = 5$, as in fig. 3), genetic divergence is very strong when viability selection acts in both sexes, and changes in divergence due to the presence of P^B are often negligible (not shown). We note, however, that regime **II** is absent when choosiness is strong enough (e.g. for $\alpha = 5$, for $s = 0.05$ or $s = 0.5$; not shown). Here, $m = 0.01$.

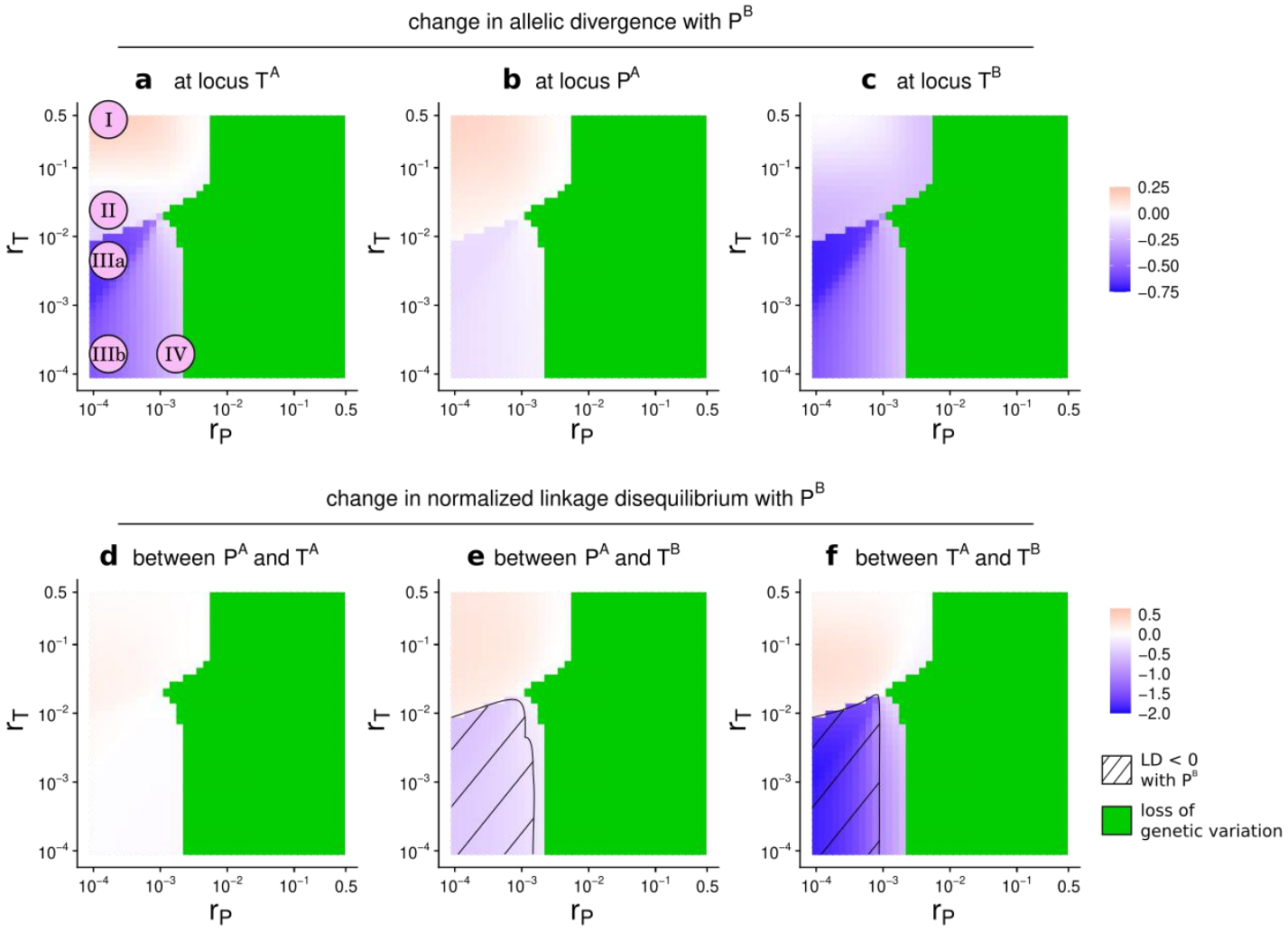

Figure S7. Comparison of equilibrium states with versus without P^B, with an alternate gene order $P^AT^AT^BP^B$. Here, recombination occurs at a rate r_{TT} between the trait loci T^A and T^B, and at a rate r_{PT} between the loci within each preference-trait set (both between loci P^A and T^A, and between loci P^B and T^B). We compare the equilibrium states with P^B versus without P^B, and represent the change in allelic divergence (**a**-**c**), the change in normalized LD (**d**-**f**), and the change in reproductive isolation (RI; **g**). See caption of figs. 2 and 4 for details. For the parameter combination tested, negative coupling occurs when recombination occurs at a lower rate within a set than between sets (for $r_{PT} > r_{TT}$, which corresponds to the case where the presence of many "recombinant" females with "mismatched" preferences increase the mating success of "recombinant" males with "mismatched" traits, as in our main analysis; **g**). This occurs through a decreased LD between the T^A and T^B loci, albeit without the establishment of negative LD between the P^A and P^B loci (**f**; primary effect (4) in tab. 1). Further theoretical studies are needed to understand how gene order determines the outcome in terms of coupling. Note that for $r_{PT} = 0.5$, we obtain the same outcome as in our main analysis for $r_P = 0.5$ (fig. 2), as in both cases, only the trait loci are physically linked with each other. Here, $s = 0.5$, $m = 0.01$ and $\alpha = 5$.